Pacific Northwest
NATIONAL LABORATORY

PNNL-30445

Degradation and Failure Phenomena of Accident Tolerant Fuel Concepts

FeCrAl Alloy Cladding

September 2020

CE Goodson
KJ Geelhood

Prepared for the U.S. Nuclear Regulatory Commission
Office of Nuclear Regulatory Research
Under Contract DE-AC05-76RL01830
Interagency Agreement: NRC-HQ-25-14-D-0001
Task Order Number: 31310018F0044 MOD P00003

DISCLAIMER

PACIFIC NORTHWEST NATIONAL LABORATORY
operated by
BATTELLE
for the
UNITED STATES DEPARTMENT OF ENERGY
under Contract DE-AC05-76RL01830

Printed in the United States of America

Available to DOE and DOE contractors from the Office of Scientific and Technical Information,
P.O. Box 62, Oak Ridge, TN 37831-0062
www.osti.gov
ph: (865) 576-8401
fax: (865) 576-5728
email: reports@osti.gov

Available to the public from the National Technical Information Service
5301 Shawnee Rd., Alexandria, VA 22312
ph: (800) 553-NTIS (6847)
or (703) 605-6000
email: info@ntis.gov
Online ordering: http://www.ntis.gov

PNNL-30445

Degradation and Failure Phenomena of Accident Tolerant Fuel Concepts

FeCrAl Alloy Cladding

September 2020

CE Goodson
KJ Geelhood

Prepared for the U.S. Nuclear Regulatory Commission
Office of Nuclear Regulatory Research
Under Contract DE-AC05-76RL01830
Interagency Agreement: NRC-HQ-25-14-D-0001
Task Order Number: 31310018F0044 MOD P00003

Pacific Northwest National Laboratory
Richland, Washington 99354

This page intentionally blank.

Abstract

The U.S. Nuclear Regulatory Commission (NRC) is anticipating licensing applications and commercial use of accident tolerant fuel (ATF) in United States commercial nuclear power reactors. Pacific Northwest National Laboratory is providing technical assistance to the NRC related to the newly proposed nuclear fuel and cladding designs.

This report focuses specifically on the iron-chromium-aluminum (FeCrAl) alloys being investigated to replace zirconium-based alloys for fuel cladding and provides current state-of-the-industry information on material properties and fuel performance considerations under reactor operating conditions and design basis accident conditions.

Currently, Global Nuclear Fuels (GNF) is the only U.S.-based fuel vendor considering FeCrAl cladding as a near-term ATF design. GNF has tested several different FeCrAl alloys including Kanthal APMT, C26M, and MA956; fueled C26M rods and unfueled Kanthal APMT, C26M, and MA956 rods have been inserted in lead test assemblies at Plants Hatch and Clinton. This report will focus on those three alloys specifically, with broader information given regarding in-reactor and ex-reactor testing of FeCrAl alloys.

To support the NRC's readiness efforts, this report will identify and discuss degradation and failure modes of FeCrAl cladding concepts, including fuel performance characteristics that may not be addressed within existing regulatory documents.

This page intentionally blank.

Acronyms and Abbreviations

AOO	anticipated operational occurrence
ASME	American Society of Mechanical Engineers
ATF	accident tolerant fuel
ATR	Advanced Test Reactor
BDBA	beyond design basis accident
BWR	boiling water reactor
CGN	China General Nuclear
CHF	critical heat flux
CILC	CRUD-induced localized corrosion
CRUD	Chalk River unknown deposit
DBA	design basis accident
DNB	departure from nucleate boiling
DNBR	departure from nucleate boiling ratio
DOE	Department of Energy
dpa	displacements per atom
ECCS	emergency core cooling system
ECR	equivalent cladding reacted
EPRI	Electric Power Research Institute
GE	General Electric
GNF	Global Nuclear Fuels
INL	Idaho National Laboratory
KAERI	Korea Atomic Energy Research Institute
KEPCO	Korea Electric Power Corporation
LANL	Los Alamos National Laboratory
LOCA	loss-of-coolant accident
LTA	lead test assembly
LTR	licensing topical report
LWR	light water reactor
MCPR	margin to critical power ratio
NRC	U.S. Nuclear Regulatory Commission
ODS	oxide dispersion strengthened
OECD-NEA	Organization for Economic Cooperation and Development – Nuclear Energy Agency
ORNL	Oak Ridge National Laboratory
PCMI	pellet-cladding mechanical interaction
PCT	peak cladding temperature

PIE	post-irradiation examination
PIRT	Phenomena Identification and Ranking Table
PNNL	Pacific Northwest National Laboratory
PWR	pressurized water reactor
R&D	research and development
RIA	reactivity-initiated accident
SAFDL	specified acceptable fuel design limit
SATS	Severe Accident Test Station
SCC	stress corrosion cracking
SRP	Standard Review Plan
SS	stainless steel
TIG	tungsten inert gas
TREAT	Transient Reactor Test

Contents

Figures

This page intentionally blank.

Tables

This page intentionally blank.

1.0 Introduction

The accident at the Fukushima Daiichi power plant led to a worldwide interest in the development of nuclear fuel systems with enhanced accident tolerance, leading to starting accident tolerant fuel (ATF) programs among industry teams and across many research institutions.

The United States Nuclear Regulatory Commission (U.S. NRC) is expecting license applications for and commercial use of ATF. Accident tolerant fuel is being developed to "improve safety in the event of accidents in the reactor or spent fuel pools" (U.S. Congress 2011) while maintaining or exceeding normal reactor operational expectations compared to current fuel technologies. The current ATF designs under development fall into one of two categories: cladding and fuel. Cladding developments include coated Zircaloy cladding, silicon carbide (SiC) cladding, and FeCrAl cladding; fuel developments include doped UO_2, high density fuels (e.g., U_3Si_2), and metallic fuels.

As most of the NRC's regulatory framework was developed for the zirconium alloy-clad, UO_2-fueled system, Pacific Northwest National Laboratory (PNNL) is providing technical assistance related to the new proposed fuel and cladding designs to enhance the staff's knowledge base and ultimately support the NRC's efforts to develop and review the required regulatory infrastructure for commercial use of ATF.

Iron-based alloys have been used as cladding since the 1950's. They were eventually replaced by zirconium-based alloys; FeCrAl (iron-chromium-aluminum) alloys are ferritic steels and exhibit better stress corrosion cracking (SCC) resistance than other steels previously used as cladding (Terrani 2018).

This report provides current state-of-the-industry information on material properties and fuel performance considerations for FeCrAl cladding in normal operating reactor conditions, design basis accident (DBA) conditions, and beyond design basis accident (BDBA) conditions. This report will also identify and discuss degradation and failure modes of FeCrAl cladding, including fuel performance characteristics of FeCrAl-clad fuel that may not be addressed within existing regulatory documents.

The scope of this report includes: an overview of the FeCrAl-related activities of each U.S.-based fuel vendor, in the U.S. national laboratories, and in other countries; an overview of the alloys GNF is considering for IronClad; cladding material properties, including those that are still needed; cladding safety limits; a literature review of available data in terms of various tests performed; and a recommendation for further testing.

1.1 Background

Cladding for light water reactors (LWRs) has historically been fabricated from zirconium alloys; Zircaloy-2 has been used for boiling water reactors (BWRs) and Zircaloy-4 has been used for pressurized water reactors (PWRs). In-reactor cladding corrosion became an issue as demand for higher burnup levels of LWR fuels grew. To reduce the issue and maintain (or improve) the creep properties of the cladding, nuclear fuel vendors developed proprietary Zr-based alloy claddings that have mostly replaced the traditional Zr-based alloys. Currently, Westinghouse uses

ZIRLO®[1] and Optimized ZIRLO™ for PWR fuel and Zircaloy-2 for BWR fuel; Framatome uses M5®[2] for PWR fuel and Zircaloy-2 for BWR fuel; Global Nuclear Fuels (GNF), only supplying BWR fuel, recently received approval for GNF-Ziron. LWR cladding is typically between 0.56 mm and 0.75 mm thick.

ATF cladding is being developed primarily to give an advantage during high-temperature steam oxidation that can occur following a DBA or in a situation considered to be beyond the fuel design basis; however, there is a general set of requirements placed on nuclear fuel cladding to retain shape, pellets, and fission products and effectively transfer heat to the coolant (10 CFR § 50, Appendix A). Prior NRC and PNNL experience in review and approval of advanced Zr-based alloy cladding will be used in the development of material for review and approval of ATF cladding.

The specific damage and failure mechanisms that have historically been identified for LWR fuel are discussed in greater detail in Section 4.0 of this report. In general, safety analyses are performed prior to operation to show:

- Rods will not fail (e.g., lose hermeticity, melt fuel pellets, or exceed other design limits) during any condition of normal operation, including during anticipated operational occurrences (AOOs)
- Fuel damage during postulated accidents will not be severe enough to prevent control rod or control blade insertion
- Fuel failures during postulated accidents will not result in dose outside acceptable limits
- There is no loss of coolable geometry.

1.1.1 Normal Operation and Anticipated Operational Occurrences

Fuel rods are static components, yet the cladding is exposed to tensile and compressive stresses and exhibits strain in several directions. Early in life the fuel/cladding gap is open, and the external pressure is much greater than the internal pressure; the cladding exhibits irradiation-assisted creep in the hoop direction, toward the fuel pellet. At some point, due to the combination of pellet outward swelling and cladding creep, the fuel/cladding gap closes. Continued pellet swelling causes the cladding to strain outward in the hoop direction. Later in life – if enough fission gases are released from the pellet – the internal pressure may exceed the system pressure and irradiation-assisted creep in the hoop direction may cause the fuel/cladding gap to reopen.

Because Zr-based alloy cladding exhibits a hexagonal crystal structure and is highly textured, radiation also causes growth in the axial direction; when the fuel/cladding gap is closed, pellet swelling in the axial direction can result in further cladding strain in the axial direction. FeCrAl alloys have body-centered cubic (BCC) structure so they are not expected to exhibit a preferential crystal orientation that would cause swelling in a particular direction. Additionally, in BCC steel, and particularly BCC steel with no nickel, has been observed to exhibit significantly less radiation swelling than face-centered cubic steel (Garner, Toloczko, and Sencer 2000).

As Zr-based alloy cladding reacts with water, a corrosion layer of ZrO_2 builds up on the cladding's outer surface. For FeCrAl alloys, the oxide layer that develops in-reactor is a thin layer of Cr_2O_3 that protects the base metal for further corrosion (see Section 4.3.2.4); for Zr-based alloys, ZrO_2

[1] ZIRLO® and Optimized ZIRLO™ are registered trademarks of Westinghouse Electric Company LLC.
[2] M5® is a registered trademark of Framatome.

does not completely protect the base metal from further corrosions, instead only slowing the reaction rate.

Light water reactor cladding is exposed to the following reactor conditions under normal operations:

Table 1-1. Reactor conditions under normal operations.

-	BWR	PWR
Coolant temperature [°F (°C)]	Water: 530-550 (277-288) Steam: 550 (288)	Water: 550-610 (288-321)
Coolant pressure [psi (MPa)]	1035 (7.1)	2250 (15.5)
Coolant mass flux [lb/ft^2-hr]	~1.05 x 10^6	~2.55 x 10^6
Fast neutron flux [n/m^2-s]	1 x10^{18}	1 x 10^{18}
Core residence time [days]	1500-2000	1500-2000
Maximum rod-average burnup [GWd/MTU]	62	62

The reactor conditions during AOOs are not significantly different than those during normal operation and typically only result in brief changes in power or coolant flow rate. These changes are less than 50% of the nominal values.

1.1.2 Design Basis Accidents

During a DBA event, failure of the cladding is permitted but dose resulting from these failures should not exceed acceptable limits and failure should not impact the coolability of the fuel assembly. The main DBAs of interest to the fuel design review are reactivity-initiated accidents (RIAs) and loss-of-coolant accidents (LOCAs), described below.

Reactivity-Initiated Accident

An RIA is caused by the rapid removal of a control rod or control blade from the core, which results in nearby fuel rods experiencing a rapid increase in power. The power excursion causes thermal expansion of the pellet which can then contact the cladding and cause relatively large (1-5%) hoop strain in the cladding at relatively low temperatures (less than 700 °C). This pellet-cladding mechanical interaction (PCMI) can cause cladding failure and, if extreme enough, can lead to expulsion of the fuel from the cladding, resulting in a loss of coolable geometry or a pressure pulse that can damage the reactor vessel.

Loss-of-Coolant Accident

In the case of a large pipe break, rapid depressurization and the complete loss of water to the reactor core can occur. In the case of a small pipe break, a slower depressurization and partial loss of water to the reactor core can occur. Although the fission process is stopped by automatic control rod insertion, this loss of active cooling leads to heating of fuel rods from decay heat. Ballooning and burst of Zr-based alloy fuel rods are observed between 800 °C and 1000 °C and high-temperature oxidation of cladding with steam, an exothermic reaction which creates additional heat, is observed between 1000 °C and 1200 °C. FeCrAl, however, has improved reaction kinetics with steam and produces hydrogen at a slower rate compared to Zr-based alloys.

At some point during the event, the emergency core cooling system will reflood the reactor with water, resulting in potential rapid cooling of the fuel rods by water quenching. Numerous mechanisms for fuel cladding failure exist in the accident, including ballooning and burst where fuel may be ejected from the fuel rods and high-temperature corrosion which could embrittle the cladding, leading to fuel fracture and a loss of coolable geometry during the reflood phase.

The oxides developed in FeCrAl alloys (chromia and alumina) differ from the zirconium oxide developed in Zr-based alloys. The difference in crystal structure (hexagonal close packed for Zr-based alloys and BCC for FeCrAl alloys) leads to texture in Zr-based alloys but none in FeCrAl alloys. Under normal operating conditions, FeCrAl alloys are protected by a thin layer of oxide rich in chromium. As the temperature increases, a thin layer of alumina develops underneath the chromia. Beyond 1100 °C, the chromia evaporates, leaving behind the thin alumina layer, which protects the material up to its melting point (~1500 °C) (Rebak 2018a). In a recent study, FeCrAl tubes failed with very little or no ballooning (Joshi et al. 2020). See Sections 4.3.2.3 and 4.3.2.4 for more details.

1.1.3 Beyond Design Basis Accidents

The Fukushima accident is considered a BDBA. In this event there was a long-term loss of offsite power and no onsite generating capacity, leading to an inability to remove decay heat from the shutdown reactor core. After an extended period, the water in the core boiled off and the cladding reacted with the steam to produce hydrogen; the hydrogen was not properly vented from the reactor building and after a critical concentration of hydrogen accumulated, an explosion occurred.

Currently the U.S. has no regulations related to fuel performance and qualification during events and accidents classified as “beyond design basis”[1]. However, FeCrAl alloys resist steam attacks above 1200 °C (Rebak, Terrani, and Fawcett 2016), up to the melting point around 1500 °C. If this resistance is realized, it may allow some performance beyond design basis.

[1] Note that the NRC has various requirements for beyond design basis accidents, including the station blackout rule (10 CFR 50.63), the anticipated transient without scram rule (10 CFR 50.62), and requirements for maintaining or restoring core and spent fuel pool cooling and containment integrity in the event of large explosions or fires (10 CFR 50.54 (hh)(2), also known as B.5.b). The NRC has also published the Mitigation of Beyond Design-Basis Events rule (84 FR 39684) governing various aspects of beyond design basis accidents that originates as part of the post-Fukushima lessons-learned activities. However, none of these rules and regulations establish specific requirements for fuel performance or qualification for beyond design basis accidents.

1.2 Previous Reviews

Three publications have been identified as providing a reasonable overview of the work that has been done to support the development of ATF:

1. The Organization for Economic Cooperation and Development – Nuclear Energy Agency (OECD-NEA) has published a state-of-the-art report on LWR ATF (OECD-NEA 2018).

2. Oak Ridge National Laboratory (ORNL) published a review paper in *Journal of Nuclear Materials* summarizing the status and challenges associated with ATF (Terrani 2018).

3. The Electric Power Research Institute (EPRI) has published a report evaluating the performance of ATF under BDBA, DBA, and AOO scenarios, with specific reference to the U.S. fleet and regulations (EPRI 2019).

OECD-NEA Report

The OECD-NEA state-of-the-art report discusses the work being done on all ATF concepts, including some development and data collection activities that have been performed. Chapter 11 of that report describes FeCrAl. The report summarizes the main advantages of and the challenges to be monitored for FeCrAl cladding:

Main advantages:

- Superior resistance to fragmentation upon reflooding in a DBA
- Increased wear resistance
- Increased reactor coping time in accident conditions
- Enhanced ability to maintain a coolable geometry in accident conditions
- Improved coolant oxidation reaction kinetics in accident conditions → significant reduction in heat generation and hydrogen generation during accident conditions
- Increased allowable peak cladding temperature (PCT) during normal operations and AOOs and in accident conditions
- Similar or better ballooning and perforation characteristics than zircaloy in accident conditions → improvement in fission product retention.

Challenges to be monitored:

- Increased parasitic neutron absorption relative to zirconium alloys
- Increased fuel pellet diameter with a reduction in cladding thickness to ~300 µm at a constant fuel enrichment of 4.9 w/o can maintain current cycle length → increased fuel cycle costs
    - No increased costs related to handling, storage, and cooling are anticipated (Rebak, Terrani, and Fawcett 2016)
- Increased permeability of hydrogen through the cladding → increased release of tritium into the reactor coolant during normal operations and AOOs
- Lack of some irradiated material properties and integral tests.

Review Article in Journal of Nuclear Materials

The article in *Journal of Nuclear Materials* (Terrani 2018) discusses the work being done on all ATF concepts, including the development status of and challenges facing the use of FeCrAl cladding. Systematic studies have been performed to determine the critical quantities of Cr and Al in the alloy system to avoid embrittlement as a result of the α'-phase precipitation that occurs after irradiation at 300 – 400 °C and to increase resistance to high-temperature steam oxidation. Normal operation and AOO behavior of FeCrAl cladding is expected to be superior to that of Zr-based cladding. However, FeCrAl cladding has a poor thermal neutron utilization factor and a potential for increased tritium release.

These conclusions help in determining if a concept should be evaluated for ATF research and does not consider the requirements for licensing of such fuel.

EPRI Report

The EPRI report (EPRI 2019) evaluated the performance of ATF under BDBA, DBA, and AOO scenarios, with specific reference to the U.S. fleet and regulations. The report presented the following potential safety benefits of FeCrAl cladding:

- Reduced fuel fragmentation and dispersal, which reduces fuel-cladding gap and in-vessel releases;
- Improved fuel reliability;
- Reduced oxidation;
- Reduced corrosion and hydrogen pickup;
- Additional coping times;
- PCT and departure from nucleate boiling (DNB) benefits, which enable improved thermal margins and increased burnups;
- Tolerance to Chalk River unknown deposit (CRUD)-induced localized corrosion (CILC);
- Improved fission product barrier in accident (DBA and BDBA) conditions, which reduces equipment qualification demands;
- Potential replacement of DNB limits with dryout; and
- Improved DBA margins, which enables thermal limit relaxation by relaxing emergency core cooling system (ECCS) injection.

2.0 Overview of FeCrAl Cladding Concept Development

FeCrAl alloys have historically been used in industrial applications where high-temperature oxidation resistance is needed. Development of FeCrAl alloys has been performed by commercial entities, national laboratories, and universities, with collaboration between the different research sectors. Both wrought FeCrAl and powder metallurgy based FeCrAl alloys are under development. Within the nuclear industry, focus has been on the wrought alloys, considered to be “nuclear grade,” which in this context means an optimized composition to perform within the full range of reactor operating conditions.

This section provides an overview of concepts that are currently being developed for ATF, with focus on those concepts that are FeCrAl-related. Of the U.S. fuel vendors, only GNF is developing a FeCrAl cladding concept. Section 2.1summarizes concepts being developed by GNF; Sections 2.2 to 2.4 summarize concepts being developed in other countries; Sections 2.5 to 2.6 summarizes concepts being developed and tested at laboratories. Although the concepts being developed outside the U.S. might not have a short-term path to U.S. licensing, the research and development (R&D) may identify relevant degradation mechanisms or data that can be applied to U.S.-license-capable concepts.

2.1 Global Nuclear Fuels

Together with General Electric (GE), GNF is working toward commercializing two near-term ATF designs: Abrasion Resistant, More Oxidation Resistant (ARMOR) cladding, a coated zirconium alloy cladding with UO_2 fuel, and FeCrAl cladding called IronClad (Fawcett 2019).

Both ARMOR and IronClad have been tested at the Advanced Test Reactor (ATR). LTAs containing unfueled, IronClad-segmented rods and ARMOR-segmented rods were irradiated at Plant Hatch, discharged in February 2020 (though one rod will go through two additional cycles). Post-irradiation examination (PIE) results are expected by January 2021. LTAs with both ARMOR and three varieties of fueled IronClad-clad rods have been installed at Clinton (GE Power 2020). Further details are provided in Section 4.3.1.1.

2.2 Japan

The Japanese ATF R&D program is developing two ATF concepts: FeCrAl strengthened by the dispersion of fine oxide particles (FeCrAl-ODS) cladding, SiC/SiC composite cladding, and doped-UO_2 fuel (Yamashita et al. 2019).

Experimental studies have been conducted to evaluate key material properties for FeCrAl-ODS cladding, including strength and ductility, corrosion resistance, tritium permeability, wear resistance, iodine SCC resistance, and weldability (T. Sato et al. 2018; Takahatake et al. 2018; Kimura et al. 2018). Sheet specimens have been tested at ORNL; LOCA tests have been conducted at ORNL as well, with FeCrAl-ODS showing excellent resistance to high-temperature steam oxidation, water quenching, and burst (Sakamoto et al. 2019).

2.3 China

The Chinese ATF R&D program, led by China General Nuclear (CGN), has developed several ATF concepts including both cladding (coated Zr alloy, FeCrAl alloys, coated molybdenum alloy,

and SiC) and fuel (high thermal conductivity UO_2) (T. Liu et al. 2018). Ex-reactor testing has determined some thermal and mechanical properties of these concepts.

No plans for irradiation tests on these concepts have been indicated.

2.4 South Korea

The Korean Atomic Energy Research Institute (KAERI) and Korea Electric Power Corporation (KEPCO) R&D programs are moving forward with developing a number of ATF concepts including surface-modified Zr (Cr alloy-coated and ODS), SiC cladding, Fe-based alloy cladding, doped UO_2 fuel, microcell-, microplate-UO_2 (high thermal conductivity ceramic and metallic) fuel and TRISO-SiC composite fuel (J. H. Yang et al. 2019; Jang 2019). FeCrAl is being investigated as a coating for Zr-based alloy cladding.

CrAl-coated Zircaloy-4 cladding, CrAl-coated FeCrAl, ceramic microcell UO_2 fuel, and metallic microcell UO_2 fuel have been tested at Halden (Szőke, McGrath, and Bennett 2017). PIE is expected for these samples (H.-G. Kim et al. 2019).

2.5 Oak Ridge National Laboratory

ORNL is researching and developing several ATF concepts: coated Zr-based cladding, FeCrAl cladding, and SiC/SiC cladding (Goldner et al. 2019).

The lab has explored the high-temperature steam oxidation resistance of commercially available FeCrAl alloys (Kanthal APMT and Alloy 33) but has also conducted many studies to optimize the chromium and aluminum contents of new FeCrAl alloys. In recent years, work has continued to not only further alloy optimization for fabricability and baseline property assessment but to also understand the effects of irradiation on the mechanical properties of FeCrAl alloys (Goldner et al. 2019).

An LTA containing C26M, a FeCrAl alloy developed by ORNL, was fabricated by GNF and inserted in Hatch Unit 1 in February 2018, discharged in February 2020. Additional rods will undergo a second cycle of irradiation. PIE, refabrication, and out-of-pile testing is planned at ORNL.

2.6 Idaho National Laboratory

Two irradiation testing campaigns are underway in the ATR at INL, testing fuel rodlets in the ATR reflector region (ATF-1 campaign) and under PWR conditions (ATF-2 campaign). See Section 4.3.1.1 for more detail. Test specimens come from all industry teams. Transient testing in the Transient Reactor Test (TREAT) facility are planned for ATF concepts from all industry teams as well (Goldner et al. 2019).

3.0 Overview of GNF FeCrAl Alloys

FeCrAl alloys consist of iron (Fe), chromium (Cr), and aluminum (Al) with minor alloying additions for various purposes. There are commercially available variants; however, the main focus of U.S. R&D programs is to develop a wrought oxidation-resistant alloy variant; the Japanese effort intends to greatly improve on the strength by pursuing ODS FeCrAl alloys (Terrani 2018).

GNF remains the only fuel vendor in the U.S. with FeCrAl cladding planned for the near term. GNF has tested several different FeCrAl alloys including Kanthal APMT, C26M, and MA956. While GNF has not publicly stated which FeCrAl alloy will be used for IronClad, the two unfueled IronClad rods irradiated at Hatch were C26M, eight fueled IronClad rods inserted in Clinton were C26M, and 16 unfueled rods inserted in Clinton were C26M, APMT, and MA956. The compositions of these three alloys are shown in Table 3-1. More detail is provided below.

Table 3-1. Compositions (by weight percent) of C26M, Kanthal APMT, and MA956 FeCrAl alloys.

Alloy	Fe	Cr	Al	Mo	Ti	C	Si	Mn	Y	Cu	Co	Ni	P
C26M[1]	Balance	12	6.0	2.0	-	-	0.2	-	0.03	-	-	-	-
Kanthal APMT[2]	Balance	20.5-23.5	5.0	3.0	-	0.08 max	0.7 max	0.4 max	-	-	-	-	-
MA956[3]	Balance	18.5-21.5	3.75-5.75	-	0.2-0.6	0.1 max	-	0.30 max	0.3-0.7[4]	0.15 max	0.3 max	0.50 max	0.02 max

[1] (Yamamoto et al. 2019)

[2] (Kanthal 2019)

[3] (Special Metals)

[4] Values given are for Y_2O_3

A detailed evaluation of each alloy variant not being considered by GNF is outside the scope of this report.

3.1 FeCrAl Design

FeCrAl alloys are fully ferritic (BCC structure) with typically no phase transformation to or from austenite (face-centered-cubic (FCC) structure) between liquidus temperature and room temperature due to the Cr and Al additive effects on Fe-based alloys (Field 2018). Cr additions contribute to corrosion resistance by forming a layer of chromium oxide (or chromia) under normal conditions; Al additions improve high-temperature oxidation resistance by forming an aluminum

oxide (or alumina) layer under accident conditions (Rebak 2018a). The Cr additions further stabilize the alumina layer in high-temperature steam.

Figure 3-1 shows the Fe-Cr binary phase diagram and indicated the formation of the brittle Cr-rich α' phase at relatively low temperatures where LWRs are operated. Al addition reduces the driving force of Cr-rich α' phase formation even in alloys with relatively high Cr contents (Field 2018; Wukusick 1966).

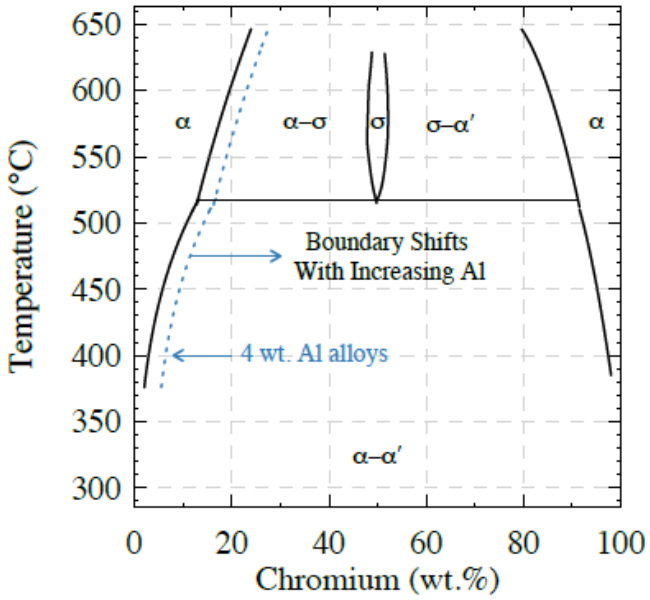

Figure 3-1. Fe-Cr binary alloy phase diagram showing phase boundaries of α-Fe, α'-Cr, and σ-FeCr. The effect of a 4 w/o Al addition on the alpha-α' phase boundary is also shown as example (Field 2018; Wukusick 1966).

The Cr and Al contents need to be balanced not only for surface protection but also for property control. If the Cr content is too high, it can lead to embrittlement as a result of the α' phase precipitation (Field 2018), as shown in Figure 3-2. Small additions of yttrium can enhance the oxidation resistance of the alloy (S. Kim, Moon, and Bahn 2019). ODS variants can have a higher strength and increased high-temperature creep resistance due to the dispersion of fine oxide particles (Yano et al. 2017).

At ORNL, alloying additions of molybdenum and niobium have been made to FeCrAl model alloys[1], intended to increase alloy strength. Mo addition increases alloy strength through solid-solution hardening; Nb addition increases alloy strength through precipitate strengthening by the formation of Fe_2Nb-type Laves phase particles (Raiman et al. 2020).

[1] FeCrAl alloys developed by ORNL are referred to as "model" alloys in literature.

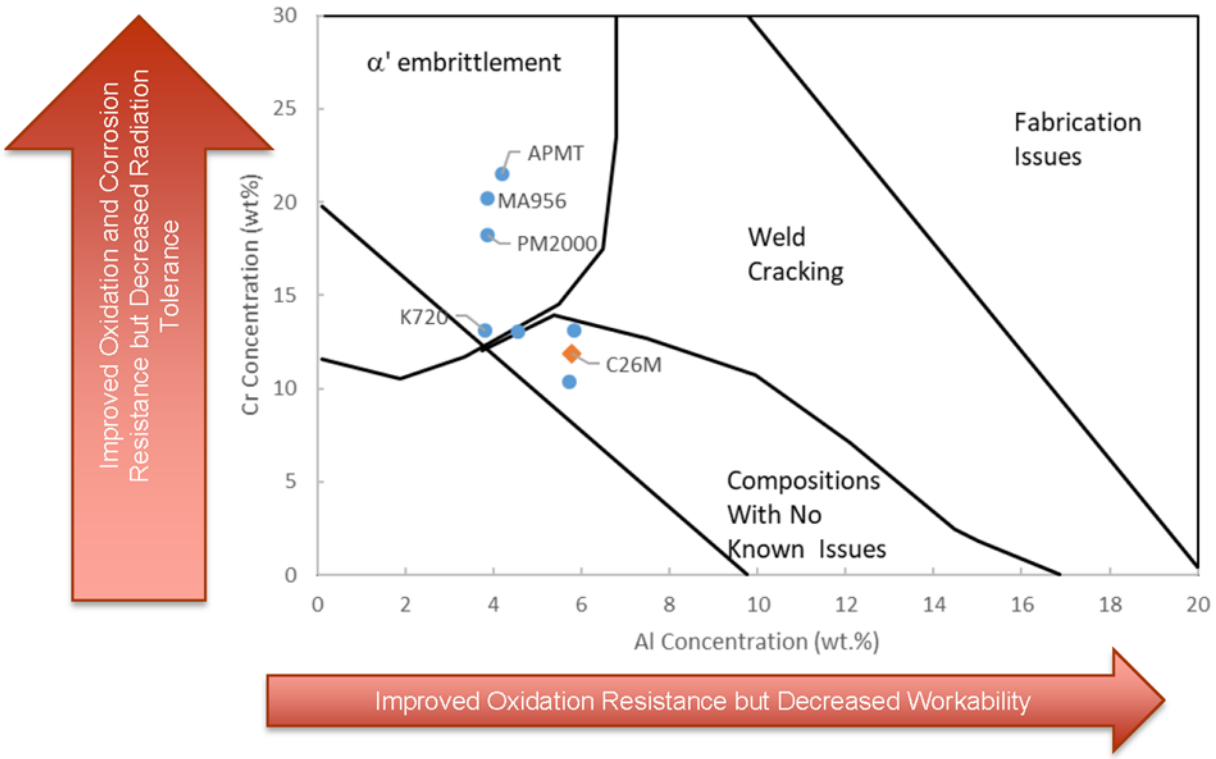

Figure 3-2. Impact of chromium and aluminum concentration in FeCrAl alloys (Yamamoto et al. 2020).

The three alloys being considered by GNF are C26M (developed by ORNL), Kanthal APMT (commercially available), and MA956 (commercially available). As seen in Figure 3-2, APMT and MA956 will likely exhibit α' embrittlement, unlike C26M, which has no known issues.

3.2 C26M

C26M is a FeCrAl alloy developed by ORNL and the subject of continual study to determine the effects of minor alloying additions, including yttrium, zirconium, cesium, carbon, and manganese (Yamamoto et al. 2019). The nominal composition is listed in Table 3-1. C26M is manufactured by traditional melting and has been fabricated into rodlets and segmented full-length rods at the industrial GNF facilities in Wilmington, NC (Richardson and Medema 2019).

The alloy is weldable by the tungsten inert gas (TIG) method, without cracks, porosity, or internal oxidation in the weld seam and no grain-boundary sensitization (Rebak et al. 2018b).

C26M has been irradiated in the ATR and Plants Hatch and Clinton (Richardson and Medema 2019). See Section 4.3.1.1 for more details.

3.3 Kanthal APMT

Kanthal APMT is a pre-oxidized commercially available ODS powder metallurgical FeCrAl alloy (Kanthal 2019) with a higher chromium content (see Table 3-1) and finer grain size (Rebak et al. 2019) than C26M.

The pre-oxidation treatment introduces a thin layer of chromia in the outer part of the alumina layer (Schuster, Crawford, and Rebak 2017). The high Cr content significantly improves the alloy's corrosion rate compared to other FeCrAl alloys (P. Wang et al. 2020; Rebak, Jurewicz, and Y.-J. Kim 2017) but as seen in Figure 3-2, Kanthal APMT is likely to exhibit α'-phase embrittlement due to the Cr and Al contents. The alloy has been exposed to high-temperature water simulating conditions of both BWR and PWR coolant conditions; the thin surface oxide layer was seen to be approximately ten times thinner than the oxide produced for Zircaloy-2 (Rebak, Terrani, and Fawcett 2016).

The alloy is weldable by the TIG method, without cracks, porosity, or internal oxidation in the weld seam and no grain-boundary sensitization (Rebak et al. 2018b).

Segmented full-length rods (non-fueled) and rodlets (fueled) have been irradiated in Clinton Cycle 20 and the ATR, respectively (Richardson and Medema 2019; Harp, Cappia, and Capriotti 2018). See Section 4.3.1.1 for more details.

3.4 MA956

MA956 is a commercially available ODS FeCrAl alloy produced by mechanical alloying (Special Metals). As seen in Figure 3-2, MA956 is likely to exhibit α'-phase embrittlement due to the Cr and Al contents.

Conventional TIG welding is possible but produces relatively low-strength joints (Special Metals).

MA956 has been irradiated in the ATR (Z. Zhang et al. 2020). See Section 4.3.1.1 for more details.

3.5 Possible Eutectics

Interactions between materials may occur during a severe accident and can contribute significantly to the general progression of the accident. Several materials must be considered for possible materials interaction with FeCrAl cladding:

- Fuel (UO_2);
- Control materials (Ag-In-Cd and B_4C);
- Burnable absorbers (e.g. Gd); and
- Various hardware such as springs, grids, and sheaths (Inconel and/or SS-304).

The interactions of FeCrAl (composition Fe-11.9Cr-6.2Al-0.50Ti-0.57Ce-0.20O) with UO_2 and B_4C have been studied at 1573 K (1300 °C) and 1673 K (1400 °C), temperatures relevant to DBA conditions (Sakamoto et al. 2016). Compared to Zircaloy-4, there was no distinct reaction between the FeCrAl-UO_2 couple. A uniform alumina layer and no clear ingress of uranium were observed. Similarly, the FeCrAl-B_4C couple showed excellent resistance to materials interaction.

The interactions of FeCrAl (Alloy B136Y, with composition Fe-13Cr-6.2Al-0.03Y) with SS-304, Inconel, and B_4C have been studied at temperatures ranging from 1300 °C to 1500 °C (Robb, Howell, and Ott 2018). These tests did not show signs of interaction for test temperatures up to 1400 °C for the FeCrAl/SS-304 combination and up to 1450 °C for the FeCrAl/Inconel and FeCrAl/B_4C combinations.

The FeCrAl/B_4C test conducted at 1500 °C appeared to have some melting of the FeCrAl; however, part of the testing apparatus fell during the experiment so the test will be repeated in the future. Fe/B_4C is known to form a low melting eutectic at approximately 1150 °C. It is postulated that a thin oxide layer protects the FeCrAl from the B_4C, which can be confirmed by future by cross-sectional micrographs.

During the QUENCH-19 test performed at Karlsruhe Institute of Technology, FeCrAl (Alloy B136Y, with composition Fe-13Cr-6.2Al-0.03Y) cladding was damaged due to probable melting or by interaction with molten SS-304 thermocouples, which have a melting temperature in the range of 1400 to 1450 °C (Stuckert et al. 2019). This could indicate eutectic interaction between FeCrAl and SS-304; however, it is possible that the cladding reached the melting point of FeCrAl as there were uncertainties in the temperature measurements and several thermocouples failed.

This page intentionally blank.

4.0 Available Data and Changes to Codes, Methods, and Limits for FeCrAl Cladding

Fuel vendors or licensees typically prepare and submit licensing topical reports (LTRs) to the NRC to describe the codes and methods required to perform bounding or cycle-specific safety analyses for a new fuel assembly design that deviates from limits applied to currently approved methodologies. Alternatively, applicants can prepare and submit supplements to existing LTRs, stating changes to the codes and methods required to perform the analyses for the new design.

This second approach has been used when introducing new proprietary cladding alloys such as ZIRLO, Optimized ZIRLO, M5, and Ziron, which are evolutionary changes from Zircaloy-2 and Zircaloy-4. These LTR supplements describe the material property correlations that will be used for the new cladding alloy along with data to justify the use of each correlation. In the case where an existing correlation will be used for the new cladding alloy, some justification, preferably citing data, that its use is appropriate should be provided. It is the applicant's responsibility to propose specified acceptable fuel design limits (SAFDLs) for their analyses and provide justification for those limits. As a result, these LTR supplements provide relevant data that demonstrate these limits will adequately protect the fuel assembly. Changes made to the analytical methodology used to perform the safety analyses for the new cladding alloy will also be described in the LTR supplement or similar licensing document.

This approach to licensing the use of a new cladding alloy can be used as a model for the introduction of FeCrAl cladding. The same review and approval will be required of any licensing requests in the following three areas:

1. Material property correlations to be used in codes for the new cladding.

2. SAFDLs for the new cladding.

3. Any changes to existing methodology.

This section is intended as a guide for the NRC staff as they perform reviews of LTRs, LTR supplements, or license amendment requests (LARs) related to the implementation of FeCrAl cladding. Section 4.1 provides an overview of the SAFDLs identified in Standard Review Plan (SRP) Section 4.2 (U.S. NRC 2007) that should be considered by an applicant. Section 4.2 identifies new damage mechanisms to be considered for FeCrAl cladding. Sections 4.3 summarizes the currently available data on FeCrAl cladding, including material properties typically needed to perform fuel thermal-mechanical analysis. Section 4.4 recommends additional testing needed to support developing and justifying limits and summarizes any remaining SAFDLs not covered in the previous sections. Section 4.5 discusses potential changes to existing codes and methodologies that may be enacted to perform safety analyses for FeCrAl cladding.

4.1 SAFDL Limits for New Cladding

NUREG-0800, Section 4.2, “Fuel System Design” (U.S. NRC 2007) identifies several general phenomena that should be considered for standard fuel and cladding to avoid fuel system damage and fuel rod failure and to ensure fuel coolability. The SRP also provides some general guidance in selecting specific limits in each area. It is the responsibility of the applicant to propose and justify the specific limit to be used in each area and to identify and propose limits for possible damage mechanisms that have not been identified by the SRP.

The SAFDLs mentioned in the SRP are broadly separated into three general categories:

1. Those related to assembly performance, typically addressed by simple calculation, manufacturing controls, and historical data
2. Those related to fuel rod performance, typically addressed for normal operation and AOOs using a thermal-mechanical code
3. Those related to fuel rod performance, typically addressed for accident conditions using a system analysis code with initial conditions provided by a thermal-mechanical code.

Table 4-1 lists each of the SAFDLs mentioned in the SRP of these categories, the purpose of each established limit, and the section of this report the limit is described in more detail.

Table 4-1. SAFDLs from NUREG-0800 and the purpose of each limit (U.S. NRC 2007).

Category	SAFDL	Purpose	Section of this Report the SAFDL is discussed
Assembly Performance	Rod bow	Could impact departure from nucleate boiling ratio (DNBR) or margin to critical power ratio (MCPR)	Section 4.4.1.1
	Irradiation growth	Excessive assembly growth could lead to assembly deformation	Section 4.3.3.1
	Hydraulic lift loads	The weight of the assembly and force of holddown springs should prevent assembly liftoff	Section 4.4.1.2
	Fuel assembly lateral deflection	Lateral deflections should not be so great as to prevent control rods/blades from being inserted	Section 4.4.1.3
	Fretting wear	Excessive fretting wear can lead to failed cladding	Section 4.3.2.5

Category	SAFDL	Purpose	Section of this Report the SAFDL is discussed
Fuel rod performance (normal operation and AOO)	Cladding stress	Prevent failure of cladding from overstress conditions	Section 4.3.2.2
	Cladding strain	Prevent failure of cladding from excessive strain conditions	Section 4.3.2.2
	Cladding fatigue	Prevent failure of cladding from cyclic fatigue	Section 4.3.3.2
	Cladding oxidation, hydriding, and CRUD	Prevent oxide spallation which can result in formation of brittle hydride lens Retain cladding ductility as stated in cladding strain limit	Section 4.3.2.4
	Rod internal pressure	Prevent cladding liftoff due to overpressure during normal operation Prevent reorientation of the hydrides in the radial direction in the cladding which can embrittle the cladding (protect strain limit) Prevent significant deformation resulting in DNB	Section 4.3.2.2
	Internal hydriding	Retain cladding ductility as stated in cladding strain limit	Section 4.4.2.1
	Cladding collapse	Prevent failure of cladding due to collapse in the plenum and axial pellet gaps which results in large local strains	Section 4.3.2.2
	Overheating of fuel pellets	Prevent fuel melting during LOCA to assure that axial or radial relocation of molten fuel would neither allow molten fuel to contact the cladding nor produce local hot spots; melting should also be precluded during RIA to reduce violent expulsion of fuel	Section 4.4.2.2
	Pellet-to-Cladding interaction	Prevent failure of cladding from chemically assisted cracking	Section 4.4.2.3

Category	SAFDL	Purpose	Section of this Report the SAFDL is discussed
Fuel rod performance (accident conditions)	Overheating of the cladding	Failure of cladding and dose consequence if critical heat flux is exceeded	Section 4.3.2.6
	Excessive fuel enthalpy	Failure of cladding and dose consequence during RIA if injected energy limit is exceeded; two limits are in place regarding maximum fuel enthalpy to evaluate fuel failure and core cooing	Section 4.3.3.1
	Bursting	Time of burst during LOCA needed for oxidation of inner cladding and associated heat is correctly modeled	Section 4.3.2.3
	Mechanical fracturing	Failure of cladding and dose consequence from external event	Section 4.3.3.1
	Cladding embrittlement	Coolable geometry must be retained following LOCA; there should be no post-LOCA general fuel/assembly failure	Section 4.4.3.1
	Violent expulsion of fuel	Coolable geometry must be retained following RIA; pressure pulse must not damage reactor vessel	Section 4.4.3.2
	Generalized cladding melting	Coolable geometry must be retained following LOCA	Section 4.4.3.3
	Fuel rod ballooning	Degree of ballooning needed to calculate blockage of the coolant channel	Section 4.3.2.3
	Structural deformation	Coolable geometry must be retained following LOCA or seismic event	Section 4.3.3.1

4.2 New Damage Mechanisms

This section also identifies new damage mechanisms that should be considered for FeCrAl cladding, which may either be addressed by applicants through existing limits or as separate limits. The following damage mechanisms have been identified through a technical review of recent data and a general understanding of cladding behavior. Each is a physical mechanism that should be addressed even if no credit for performance is credited in the fuel system safety review.

4.2.1 Radiation Effects on FeCrAl

Irradiation of FeCrAl cladding may result in several products of neutron activation. Neutron irradiation of Cr-50 (4.4 a/o abundant in natural Cr) will result in Cr-51, a radioisotope with a half-life of approximately 28 days. Neutron irradiation of Al-27 (100 a/o abundant in natural Al) will result in several activation products:

- $^{27}Al + n \rightarrow {}^{28}Al$; Al-28 beta decays (half-life 2.28 minutes) to the excited state of Si-28, which de-excites via gamma emission to stable Si-28
- $^{27}Al(n,p)^{27}Mg$; Mg-27 beta decays (half-life 9.45 minutes) to two excited states of Al-27, both of which de-excite via gamma emission to stable Al-27
- $^{27}Al(n,\alpha)^{24}Na$; Na-24 beta decays (half-life 15 hours) to the second excited state of Mg-24, which de-excites via gamma emission to the first excited state of Mg-24, de-exciting via gamma emission again to stable Mg-24
- $^{27}Al(n,2n)^{26}Al$; Al-26 beta decays (half-life 7.2E5 years) to the excited states of Mg-26, which de-excite via gamma emission to stable Mg-26

These isotopes will be formed but it is not known if they will be released to the coolant in significant quantities; release to the coolant could challenge the plant dose release limit or the ability of the chemical and volume control system to eliminate Cr or Al ions before they plate out on any reactor components.

Neutron capture of Fe-54 (~5.8 a/o abundant in natural Fe) results in Fe-55, which has a half-life of 2.75 years. Neutron capture of Fe-56 and Fe-57 result in Fe-57 and Fe-58, respectively, both stable isotopes. Neutron capture of Fe-58 results in Fe-59, a radioisotope that decays by beta and high-energy gamma emission; however, the abundance of Fe-58 in natural iron is 0.28 a/o.

The formation and possible release of these activation products may be monitored through ongoing surveillance at the plant; this process is already in place to evaluate radioisotopes and gaseous and liquid effluents and is reported to the NRC on a yearly basis. If these activation products begin to challenge plant dose release limits, it will be seen to increase as more of the core inventory is transitioned to FeCrAl cladding. In this case, systems can be implemented to effectively remove these activation products before safety is compromised.

Additionally, a surveillance plan to monitor Cr and Al ions in the coolant chemistry can be put in place alongside the implementation of FeCrAl cladding to mitigate any impact of the ions.

4.2.2 Galvanic Corrosion

Galvanic corrosion occurs when two or more dissimilar materials are coupled in an electrolyte (i.e., brought into electrical contact under water). It can be accelerated under the effects of irradiation, as has been observed with the so-called “shadow corrosion” seen between BWR

channel boxes and control blades. When a galvanic couple forms, one of the metals in the couple becomes the anode and corrodes faster than it would by itself, while the other become the cathode and corrodes slower than it would alone.

Dissimilar metals in this case include: FeCrAl and Zr; FeCrAl and Inconel; FeCrAl and SS-304. No indication of galvanic corrosion, irradiation-assisted or otherwise, between these systems has been found in this effort. LTA data may be used to further clarify if this will be a problem for FeCrAl cladding.

4.2.3 Defects

It is currently unknown what sort of manufacturing checks will result in quality tubes of FeCrAl. As such, it is unknown what defects, let alone their size and concentration, will be introduced in the manufacturing process. Each process in question should define the allowable defects and justify their presence based on testing of cladding with similar defect concentrations.

4.2.4 Tritium Release

While not a safety concern, the high mobility of tritium in FeCrAl results in the ability for it to permeate from the fuel, through the cladding, to the coolant, potentially causing dose concerns during plant operation. Tritium permeation has been investigated for a range of different FeCrAl alloys; in general, the higher-Cr content alloys show lower permeability than the lower-Cr content alloys. There is also a significant difference in the permeability between oxidized and non-oxidized materials. Al_2O_3 has been shown to have nearly one order of magnitude lower permeability than bare FeCrAl alloys (J. T. Bell et al. 1979).

4.3 Currently Available Data

This section describes the data currently available on FeCrAl cladding, including material properties typically needed to perform fuel thermal-mechanical analysis, to develop and justify the limits listed in Table 4-1. The presence of data in any area does not indicate that an applicant would not have to provide data from their specific FeCrAl alloy because some properties may be composition dependent. These data are compiled here to give the NRC staff the expected performance of FeCrAl cladding, as well as areas of concern that should be given added scrutiny during the review of one of these concepts.

Table 4-2 summarizes the tests that could be performed to quantify material properties.

Table 4-2. Tests to quantify material property correlations for FeCrAl cladding.

Property	Recommended Tests
Thermal conductivity	Tests on unirradiated cladding samples over representative temperature range
Thermal expansion	Tests on unirradiated cladding samples over representative temperature range
Emissivity	Tests on unirradiated cladding samples (both oxidized and unoxidized) over representative temperature range
Specific heat	Tests on unirradiated cladding samples over representative temperature range
Elastic modulus	Tensile tests on irradiated cladding tubes over a representative range of burnup and temperatures
Yield stress	Tensile tests on irradiated cladding tubes over a representative range of burnup and temperatures
Thermal and irradiation creep	In-reactor creep tests on pressurized cladding tubes over a representative range of burnup and temperatures
Axial irradiation growth	Poolside length measurements from LTAs over a representative range of burnup and temperatures
Oxidation rate	Poolside eddy current measurements from LTAs over a representative range of burnup and temperatures
Hydrogen pickup	Destructive examination of cladding segments from LTAs
High-temperature ballooning behavior	Ex-reactor burst tests at relevant temperature; unirradiated samples are acceptable
High-temperature steam oxidation rate	Ex-reactor burst tests at relevant temperature; unirradiated samples are acceptable

Table 4-3 provides a summary of the tests that could be performed to justify the SAFDLs discussed in Section 4.1 beyond what is necessary to quantify the material property correlations.

Table 4-3. Tests that could be used to establish SAFDLs for FeCrAl cladding tubes beyond those needed to quantify basic material properties.

SAFDL	Recommended Tests
Rod Bow Evaluation	Testing or assessments of LTAs to ensure rod bow is not a concern for thin-walled FeCrAl
Irradiation Growth	Assessments of LTAs to determine axial irradiation growth
Fretting	Ex-reactor tests on unirradiated tubes and grids to demonstrate no damage to either part
Cladding strain/ductility	Ex-reactor tests on irradiated tubes to confirm ductility requirements in strain limits at AOO temperatures
Cladding fatigue	Ex-reactor tests on irradiated tubes to establish fatigue design curve
Thermal limits (DNB, CHF) if surface roughness is different from Zr-based alloy tubes	Ex-reactor tests on unirradiated tubes to establish thermal limits (CHF)
Excessive fuel enthalpy	Ex-reactor tests on irradiated tubes to confirm ductility requirements at RIA temperatures RIA tests or surrogates such as rapid heating and loading on irradiated fuel segments in test reactor could be used to develop RIA failure criteria
Cladding embrittlement	Ex-reactor balloon/burst/bend tests on unirradiated and/or irradiated tubes to confirm existing embrittlement limits or develop new embrittlement limits

These data can be grouped into 1) data that need to be collected in-reactor, during a poolside examination, or during PIE, 2) data that may be collected on unirradiated cladding samples, and 3) data that must be collected on previously irradiated cladding samples. The data (or lack of data) in each of these categories are discussed in the following sections.

4.3.1 In-Reactor Data

Recommended qualification data from an in-reactor test program are:

1. Thermal and irradiation creep behavior
2. Axial irradiation growth
3. Oxidation rate
4. Hydrogen pickup
5. Rod bow evaluation
6. RIA test
7. Fuel centerline temperature
8. Rod internal pressure and void volume
9. Cladding permanent hoop strain following a power ramp.

4.3.1.1 Current Irradiation Tests

This section discusses the current irradiation tests at several reactors and test facilities.

Advanced Test Reactor

The ATF-1 campaign at the ATR was intended to determine the feasibility of irradiation tests on drop-in capsule experiments and to demonstrate fabricability and viability for the ATF-2 water loop testing. ATF-1 capsules were not exposed to the ATR primary coolant system; rodlets are encapsulated in stainless steel. ATF-2 is a continuation of ATF-1, testing fuel system concepts under conditions prototypic of PWRs to demonstrate concept viability. Experiments are, or will be, discharged from the ATR and undergo PIE and/or transient testing in the TREAT facility.

As part of the ATF-1 campaign, the ATF-18 capsule contained UO_2 fuel clad in C35MN in a rodlet designated LOCA-1, a FeCrAl alloy developed by ORNL, and was irradiated to approximately 10 GWd/MTU to create irradiated samples for ORNL's Severe Accident Test Station (SATS). However, the rodlet was breached during testing and may not be an ideal candidate for further testing in SATS (Harp, Cappia, and Capriotti 2018).

Four additional capsules (ATF-06, ATF-08, ATF-45, and ATF-73) in the ATF-1 campaign contained FeCrAl cladding. ATF-06 (concept lead GE) contained UO_2 clad with Alloy 33 and was irradiated to 18.3 GWd/MTU; ATF-08 (concept lead GE) contained UO_2 clad with Kanthal APMT and was irradiated to 18.3 GWd/MTU; ATF-45 (concept lead Los Alamos National Laboratory (LANL)) contained U_3Si_2 clad with Kanthal AF and was irradiated to 13.2 GWd/MTU; ATF-73 (concept lead ORNL) contained discs of UO_2 against discs of different FeCrAl alloys for a fuel-cladding interaction test and was irradiated to 8.7 GWd/MTU (Murdock 2018). Visual inspections, neutron radiography, and gamma spectrometry have been performed on these capsules (Harp, Cappia, and Capriotti 2018). The ATF-1 experiments were run in a dry environment and, therefore, coolant-cladding interactions cannot be assessed; assessment of cladding creep down under irradiation is limited (Field 2018).

PIE has been performed on the ATF-06 and ATF-08 capsules, focusing on fuel microstructure, fuel-cladding interaction, and irradiation-induced variations of cladding mechanical properties. No

significant changes in the cladding hardness were measured and the cladding hoop strain remained limited (Cappia 2019).

Non-destructive and destructive PIE performed on the ATF-45 capsule indicated very low fission gas release; further data related to the cladding is currently unavailable (Cappia and Harp 2019).

ORNL performed PIE on the ATF-73 capsule; localized defects, namely circular pitting and cracks of a few tenths of microns, were observed on the FeCrAl disc surfaces, though these defects might be surface fabrication defects rather than irradiation-induced localized corrosion. Chemical analyses are needed to determine whether accumulation of corrosive fission products are causing enhanced interaction (Cappia and Harp 2019).

MA956 was irradiated in the ATR at 328 °C up to 4.36 dpa with both thermal and fast neutrons. Microstructures were examined before and after irradiation to estimate the swelling rate, which was determined to be 0.08% without subtracting pre-existing argon bubbles (Z. Zhang et al. 2020).

FeCrAl cladding is included in the ATF-2 campaign, currently underway; rodlets are being irradiated and exposed directly to a water loop that mimics the water chemistry condition of normal PWR operations including borated water at 350 °C and 200 psi. In situ instrumentation includes fuel centerline temperature, rod gas pressure, rod growth extensometer, pellet stack extensometer, and coolant water electrical potential (Le Coq, Martin, and Linton 2019; Bays et al. 2018). There are plans to discharge some FeCrAl rodlets before the ATR Core Internal Change shutdown, with PIE starting end of FY2021 (F. Cappia, pers. comm.).

Argonne National Laboratory

In 1967, GE irradiated FeCrAl-Y alloys and observed strength increased somewhat with increasing chromium and aluminum contents up to 750 °C, though none were as high as austenitic steel. Stress-rupture tests indicated lower stress-rupture strength than that of austenitic steels. It was determined that they possessed superior tensile yield strength up to 750 °C (GE 1968).

Engineering Test Reactor

In 1965, GE irradiated four pre-oxidized FeCrAl-Y alloys (called 1541, 2541, 0561, and 1041) to 9.25E19 n/cm^2 (E ≥ 1 MeV) in the Engineering Test Reactor at ambient temperature to measure changes in ductility and resistivity. Further studies examined tensile strength of irradiated samples and it was observed that irradiation decreased the strength, but ductility was unaffected. Effects of irradiation appeared to be removed after annealing at a temperature of about 350 °C (GE 1966).

High Flux Isotope Reactor

A series of capsules with two FeCrAl alloys, C06M and C36M, were irradiated at the High Flux Isotope Reactor (HFIR) at target temperatures of 200 °C, 330 °C, and 500 °C up to target damage doses of 8 dpa and 16 dpa for a total of six irradiations. Post-irradiation fracture toughness was measured; a slight change in the Master Curve fracture toughness transition temperature from the unirradiated condition was observed for irradiations at 501 °C/6.6 dpa and 315 °C/7.9 dpa. Significant irradiation embrittlement was observed for both alloys for the irradiation at 166 °C/6.6 dpa (Chen et al. 2019). These irradiations are intended to bookend C26M (i.e., C26M

has a 12% Cr content; C06M has a 10% Cr content and C36M has a 13% Cr content). Data gathered from the irradiations at 16 dpa have not been reported.

Various FeCrAl alloys were irradiated for the entire duration of HFIR cycle 450b to an estimated neutron fluence of 2.0E25 n/m^2, corresponding to a nominal dose level of 1.8 dpa. The response of FeCrAl alloys to radiation were similar to Fe-Cr alloys, for which more detailed data already exists (Field et al. 2015).

A study focusing on the mechanical properties of ORNL FeCrAl alloys and Kanthal APMT irradiated samples up to 13.8 dpa at irradiation temperatures between 320 and 382 °C. Radiation hardening and embrittlement indicative of high-Cr ferritic alloys have strong Cr-composition dependencies at lower doses. At and above 7.0 dpa, the mechanical properties saturated for all alloys (Field et al. 2017).

C35M and other variants were irradiated in the HFIR at 1.8-1.9 dpa in a temperature range of 195 to 559 °C. Tensile tests with digital image correlation, scanning electron microscopy-electron back scatter diffraction analysis, fractography, and X-ray tomography analysis were performed. Both as-received and welded material revealed a high degree of radiation-induced hardening for low-temperature irradiation; irradiation at high-temperature had little overall effect on the mechanical performance (Gussev, Cakmak, and Field 2018).

OECD Halden Reactor Project

Irradiation of FeCrAl rodlets containing UO_2 fuel was carried out under prototypical PWR conditions as part of IFA-796. The target burnup of ~40 MWd/kg UO_2 (Szőke, McGrath, and Bennett 2017) was not reached; the rodlet reached a peak burnup of 4.5 MWd/kg UO_2 when Halden was permanently closed in summer of 2018. The goal of the study was to demonstrate that FeCrAl could meet performance and reliability requirements under normal LWR operation, including corrosion and dimensional behavior, and the rodlets were continuously monitored for PCMI (Szőke, McGrath, and Bennett 2017). No major defects were found after one cycle (during routine interim inspection) (Field 2018).

Lead Test Assemblies

This section describes the results from LTAs.

Hatch Unit 1 Cycle 29

LTAs containing unfueled IronClad-segmented rods were irradiated at Plant Hatch, a BWR in Georgia, from February 2018 to February 2020 (though one C26M rod will go through two additional cycles). Proposed PIE includes:

1. Visual examination to characterize external surface of as-irradiated rod
2. Leak tightness test of as-irradiated rod
3. Optical and electron microscopy to assess corrosion layer thickness, composition, and metal loss
4. Mechanical properties tests to assess strength and ductility characteristics, as well as fracture toughness
5. Cyclic loading tests to assess fatigue life

6. Biaxial creep testing to assess time-dependent deformation under load
7. High-temperature oxidation testing to assess response to simulated LOCA conditions
8. Annealing tests to assess irradiation damage recovery kinetics.

RIA tests will be conducted at INL's TREAT facility to determine if the mechanical performance of C26M has a strong dependence on strain rate and establish a capability to evaluate an irradiated material's PCMI response (Brown et al. 2020).

Initial results are expected January 2021 (Le Coq, Martin, and Linton 2019).

Clinton Cycle 20

LTAs containing fueled IronClad rods have been installed at Clinton (GE Power 2020) and are currently being irradiated. PIE results will be provided at a later date.

4.3.2 Ex-Reactor Data Collected on Unirradiated Samples

Recommended qualification data from ex-reactor tests on unirradiated samples are:

1. Thermal conductivity
2. Thermal expansion
3. Specific heat and enthalpy
4. Ballooning
5. High-temperature oxidation
6. Fretting
7. Thermal limits (DNB, CHF)
8. LOCA post-quench ductility.

The following will describe the available data and overall observations and the limits and material properties the data supports.

4.3.2.1 Thermal Properties

Limited studies on the thermal properties of non-commercial FeCrAl alloys, especially lean-Cr content, have been completed. Further tests are recommended on unirradiated cladding samples over a representative temperature range. For emissivity tests, it is recommended to test both oxidized and unoxidized samples.

Table 4-4. Summary of unirradiated thermal property testing for FeCrAl cladding.

Lead	FeCrAl Alloy(s)s	Test Description	Results
ORNL (Field 2018)	Kanthal APMT C06M C35M C36M	Differential scanning calorimetry, laser flash testing, dilatometry	Specific heat capacity, thermal diffusivity, thermal expansion
ORNL (Yamamoto et al. 2019)	C26M	Dilatometry, differential scanning calorimetry, and laser flash testing	Thermal expansion, heat capacity, and thermal diffusivity

The following sections compare the thermal properties of FeCrAl alloys (C26M, Kanthal APMT, MA956, and/or a generalized correlation where applicable) to the thermal properties of Zr-based alloys.

Material Property: Thermal Conductivity

Figure 4-1 shows the thermal conductivity of Zr-based alloys (Geelhood et al. 2020) and various FeCrAl alloys (Field 2018; Special Metals). This plot does not include C26M, but recent thermal diffusivity data (Yamamoto et al. 2019), used to determine thermal conductivity, indicates that C26M will have similar thermal conductivity to these other alloys.

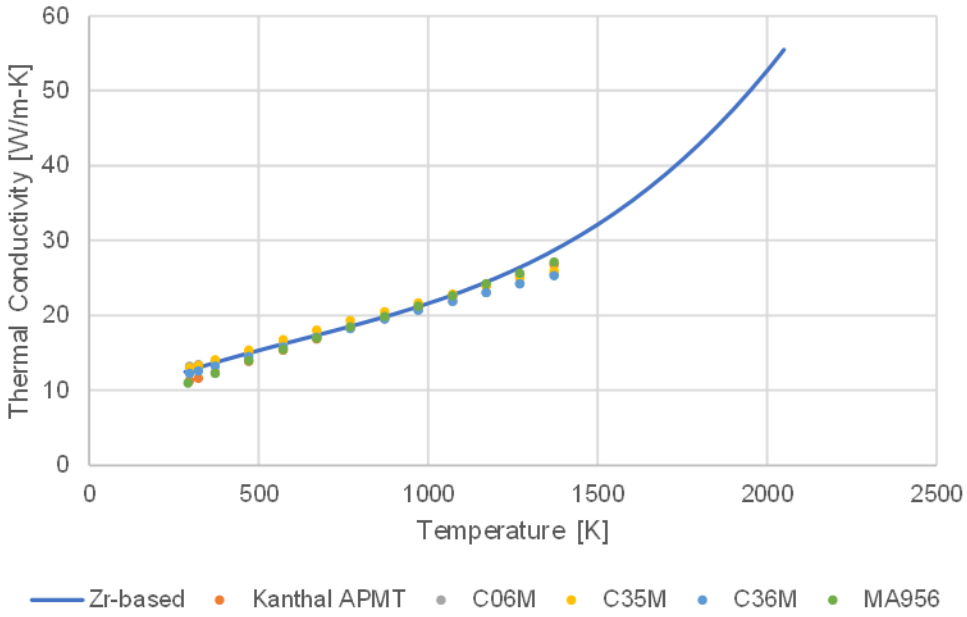

Figure 4-1. Thermal conductivity of Zr-based alloys (Geelhood et al. 2020) and various FeCrAl alloys (Field 2018; Special Metals).

The FeCrAl data (Field 2018) were collected from unirradiated samples and fit to a curve.

Material Property: Thermal Expansion

Figure 4-2 shows the thermal expansion of Zr-based alloys (Geelhood et al. 2020) and various FeCrAl alloys (Field 2018; Yamamoto et al. 2019; Special Metals). Zr-based alloy tubes are processed in such a way that the tubes exhibit a large degree of microstructural texture, which results in different thermal expansion in different directions (i.e., axial and circumferential). Recent data from C26M is included (Yamamoto et al. 2019) and shows good agreement with other FeCrAl alloys.

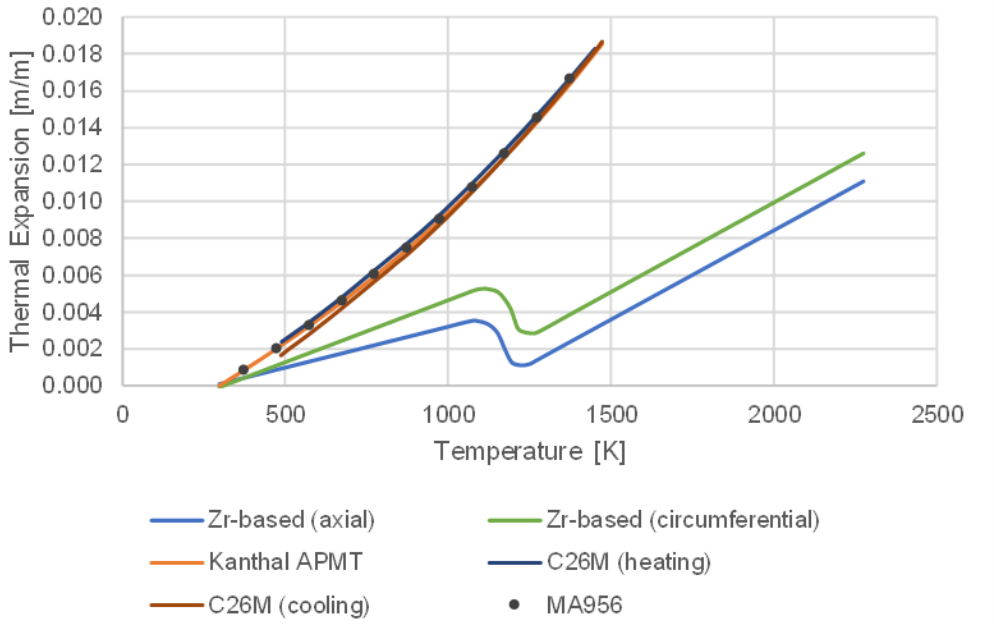

Figure 4-2. Thermal expansion of Zr-based alloys (Geelhood et al. 2020) and various FeCrAl alloys (Field 2018; Yamamoto et al. 2019; Special Metals).

C26M exhibits some differences in heating and cooling but the magnitude of this difference is not large. At lower temperatures (<1000 K), variation in the thermal expansion coefficient of FeCrAl alloys can be observed with composition (Field 2018). The FeCrAl data were collected from unirradiated samples; Kanthal APMT data were fit to a curve, but the C26M and MA956 data reported here are from direct measurements of thermal diffusivity.

As the thermal expansion of FeCrAl is higher than that of Zr-based alloys, the process of gap closure will be delayed and gap conductance increased; fuel centerline temperature will increase until the gap begins to close. This may put off and reduce the severity of PCMI, but could lead to more fission gas release early in life.

Material Property: Emissivity

Cladding emissivity is important to calculate the radiative portion of gap heat transfer and heat transfer from the outer surface of the fuel rod when unwetted, such as during a LOCA event or during film boiling. Emissivity is impacted by surface conditions, including any oxide on the surface of the cladding. Figure 4-3 shows the emissivity of fully oxidized Zr-based alloys (Geelhood et al. 2020) and Kanthal APMT (Kanthal 2019), also fully oxidized. Fully oxidized surfaces have higher emissivity than non-oxidized surfaces.

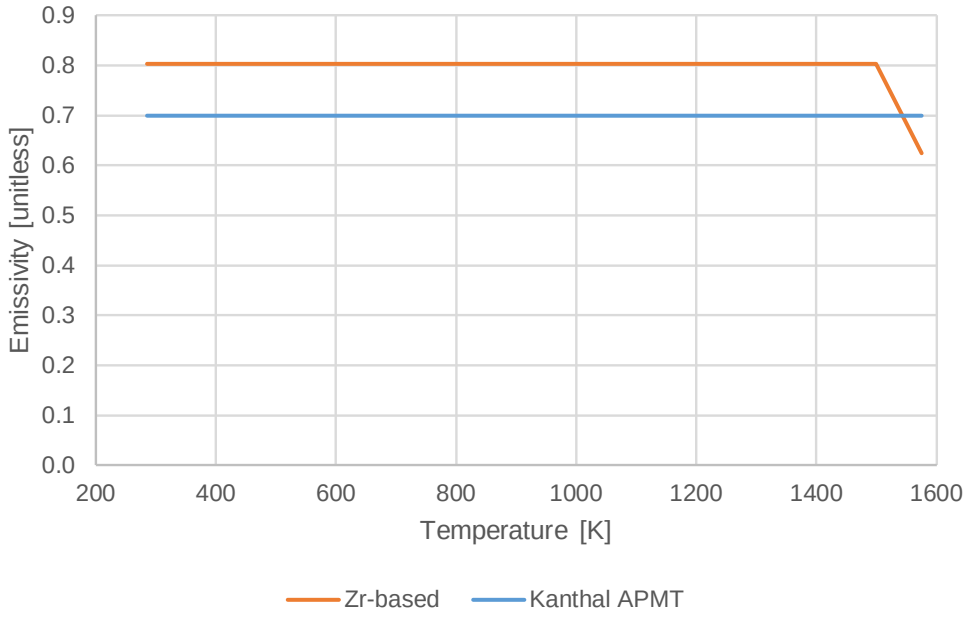

Figure 4-3. Emissivity of Zr-based alloys (Geelhood et al. 2020) and Kanthal APMT (Kanthal 2019).

Below temperatures of 1540 K (~1267 °C), the emissivity of fully oxidized FeCrAl is less than that of a fully oxidized Zr-based alloy. However, a study on the sensitivities of the parameters for gap conductance determined that, for the BISON fuel performance code, emissivity had the smallest impact on the heat transfer in the fuel-cladding gap for a UO_2/Zircaloy-2 system (Schmidt et al. 2014). As mentioned above, further testing to determine the emissivity for both oxidized and unoxidized FeCrAl alloy cladding is needed.

Material Property: Specific Heat Capacity

Figure 4-4 shows the specific heat of Zr-based alloys (Geelhood et al. 2020) and various FeCrAl alloys (Field 2018; Yamamoto et al. 2019; Special Metals). Recent data from C26M is included (Yamamoto et al. 2019) and shows good agreement with other FeCrAl alloys.

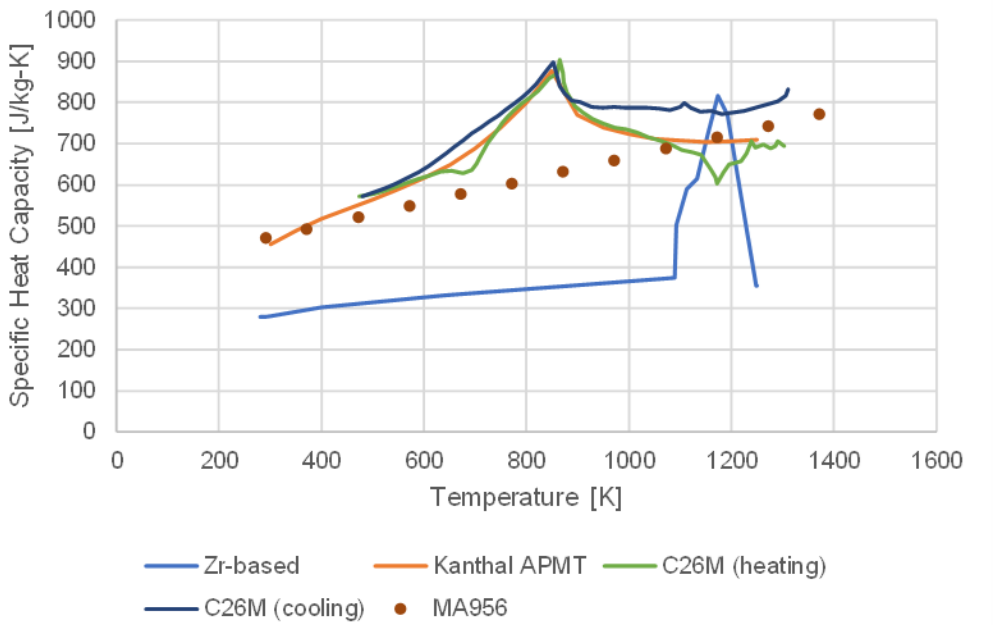

Figure 4-4. Specific heat of Zr-based alloys (Geelhood et al. 2020) and various FeCrAl alloys (Field 2018; Yamamoto et al. 2019; Special Metals).

C26M exhibits some difference between heating and cooling but both peaked around 850 K. The large peaks for C26M and Kanthal APMT correspond to the second order phase transitions from the materials' ferromagnetic to paramagnetic states. The FeCrAl data were collected from unirradiated samples; Kanthal APMT data were fit to a curve but the C26M and MA956 data reported here are from direct measurements.

4.3.2.2 Mechanical Properties

Limit: Cladding Stress

Cladding stress limits are typically set using a method described in Section III of the American Society of Engineers (ASME) code (ASME 2017) and are usually based on unirradiated yield stress to represent the lowest yield stress. For FeCrAl, the use of the unirradiated yield stress should be acceptable to determine a stress limit; Figure 4-9 shows that irradiation increases yield stress relative to the unirradiated condition.

Limit: Cladding Strain

There are two cladding strain limits that are typically employed. The first is a steady-state limit on the maximum positive and negative deviation from the unirradiated conditions that the cladding may deform throughout life. The second is a transient limit on the maximum strain increment caused by a transient and may also be applicable to accident analysis.

These cladding strain limits are typically justified based on mechanical tests (axial tension tests and tube burst tests) performed on irradiated cladding tubes. Ductility decreases with irradiation (Field et al. 2017), so these tests are most relevant when performed at the maximum expected fast neutron fluence. The uniform elongation has been typically used as the strain capability for Zr-based alloys (Geelhood, Beyer, and Cunningham 2004). This would be a good metric for FeCrAl cladding to protect against cladding mechanical failure.

Limit: Cladding Collapse

Cladding collapse in modern nuclear fuel rods has been mitigated by pellet design features such as dishes and chamfers on the ends of the pellet that effectively eliminate axial gaps in the fuel pellet column. Still, cladding collapse analyses are performed for potential small axial gaps between pellets and in the upper plenum region. The key input into this analysis is the cladding creep rate.

Limit: Fuel Rod Internal Pressure

There are several possible limits for rod internal pressure that are discussed in NUREG-0800 Section 4.2 (U.S. NRC 2007). The first and most straightforward is that the rod internal pressure shall not exceed the coolant system pressure. No outward deformation is possible if the stress in the cladding is in the compressive direction. This situation does not change with a change in cladding material and, therefore, this limit would still be applicable to FeCrAl cladding.

Greater rod internal pressures may be justified based on the following criteria:

- No cladding liftoff during normal operation
- A description of any additional failures resulting from DNB caused by fuel rod overpressure during transients and postulated accidents.

It has typically been determined by applicants with Zr-based alloy cladding that the first of these criteria is the most limiting. This should be confirmed by applicants with a FeCrAl cladding to still be the case. If so, the pressure limit where cladding liftoff could occur is typically set as the pressure where the upper bound cladding creep rate will exceed the lower bound fuel pellet

swelling rate. For FeCrAl cladding, the fuel pellet swelling rate will remain the same despite the increased pellet diameter; cladding creep rate will be determined as discussed below.

Testing: Mechanical Properties

The mechanical properties of unirradiated FeCrAl alloys have been extensively tested. All alloys show similar trends with temperature; however, the possibly composition-dependent correlations for peak stress, yield stress, and Young's modulus should be investigated further.

Table 4-5. Summary of unirradiated mechanical property testing for FeCrAl cladding.

Lead	FeCrAl Alloy(s)s	Test Description	Results
ORNL (Yamamoto et al. 2015)	T35Y2 C35M C35MC C35MNC C35MN C35MN5	Tensile tests at 24 °C and 279 °C	Yield stress, ultimate tensile stress, uniform plastic elongation, total plastic deformation
ORNL (Massey et al. 2016)	C35M	Tensile tests at 800 °C with an applied stress of 20 and 26 MPa	FeCrAl exhibited a steady-state creep rate roughly two orders of magnitude smaller than Zircaloy-4
University of Science and Technology Beijing (He et al. 2018)	Fe-20Cr-3Al Fe-20Cr-4Al Fe-20Cr-6Al	Hot tensile tests at intervals of 100 °C between 700 °C and 1200 °C	Peak stress and yield stress increased with increased Al content; Young's modulus found to decrease with increasing Al content; hot ductility more dependent on temperature than Al content
ORNL (Yamamoto et al. 2019)	C26M	Tensile test at room temperature Ramp test with a flowing steam environment to 1400 or 1450 °C	Yield strength, ultimate tensile strength, uniform plastic elongation, tensile elongation Oxidation resistance with various added alloys; excess total amounts of reactive elements could negatively impact both the oxidation resistance and the potential mechanical property degradation at elevated temperatures
University of Tennessee / ORNL (Brown et al. 2020)	C26M	Pulse-controlled modified burst test	Failure hoop strain for LWR hot zero power RIA conditions

The following sections compare the mechanical properties of FeCrAl alloys (C26M, Kanthal APMT, MA956, and/or a generalized correlation where applicable) to the thermal properties of Zr-based alloys.

Material Property: Unirradiated Yield Stress

Figure 4-5 shows the yield stress of unirradiated Zr-based alloys (Geelhood et al. 2020) and various FeCrAl alloys: C25M and Kanthal APMT (Field 2018), MA956 (Special Metals), and C26M (Yamamoto et al. 2019).

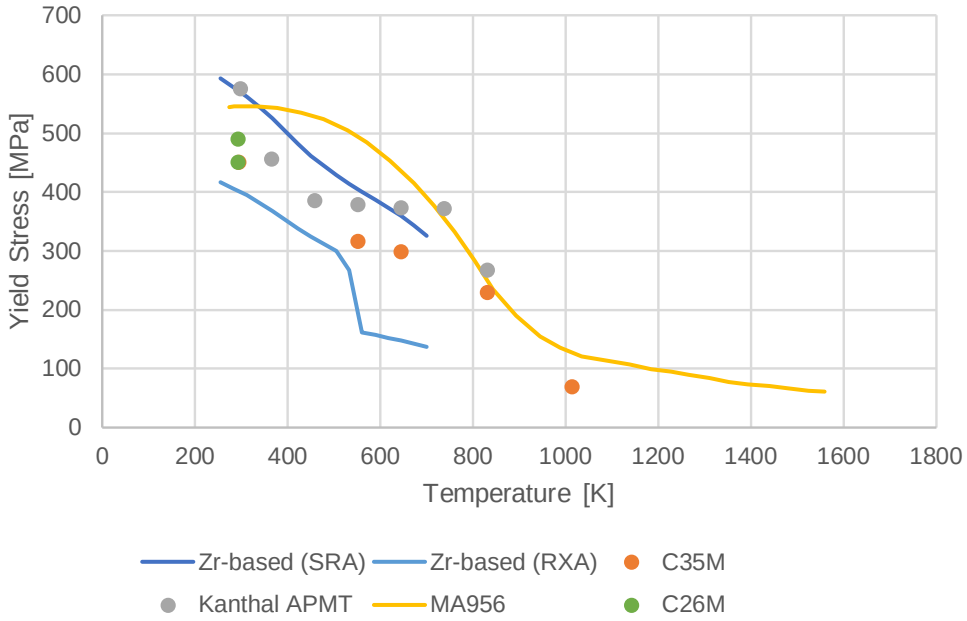

Figure 4-5. Unirradiated yield stress for Zr-based alloys (Geelhood et al. 2020) and various FeCrAl alloys (Field 2018; Special Metals; Yamamoto et al. 2019).

Given the scatter in FeCrAl yield stress, alloy- and temperature-dependent yield stress data is necessary for characterizing mechanical performance.

Material Property: Elastic Modulus

Figure 4-6 shows the elastic modulus of Zr-based alloys (Geelhood et al. 2020) and various FeCrAl alloys (Field 2018; Kanthal 2019; Special Metals).

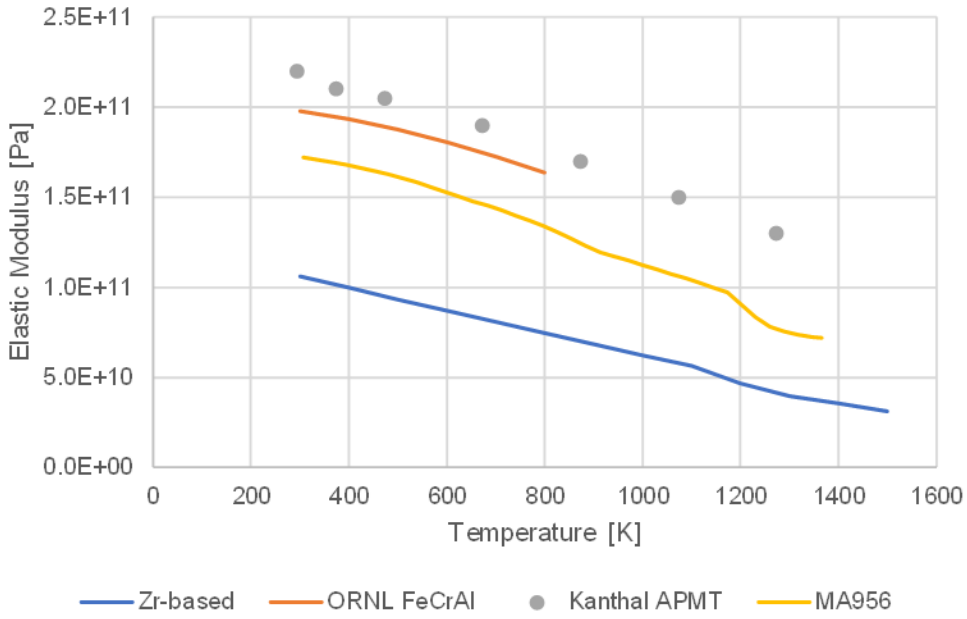

Figure 4-6. Elastic modulus of Zr-based alloys (Geelhood et al. 2020) and various FeCrAl alloys (Field 2018; Kanthal 2019; Special Metals).

Material Property: Thermal Creep Rate

It is difficult to compare thermal creep properties of Zr-based alloys and FeCrAl alloys as data exist at different temperature intervals. Zircaloy data extends up to 538 °C, while data for Kanthal APMT and MA956 start at 800 °C. Tensile tests have shown that the steady-state creep rate of unirradiated C35M is roughly two orders of magnitude smaller than that of Zircaloy-4 (Massey et al. 2016).

A generalized model for all FeCrAl alloys was presented in the Handbook on Material Properties of FeCrAl Alloys (Field 2018) for a temperature range of 350-1200 °C but further tests would be required to determine the specific creep properties of any chosen alloy in the correct temperature-stress regime.

4.3.2.3 Ballooning and Bursting

Limit: Ballooning and Bursting

Ballooning and bursting of the fuel rod relates to failure of fuel rods due to high temperatures and high gas pressures during a LOCA (and can also be a consideration during an RIA). It is important to know the rupture stress as a function of temperature and the amount of ballooning that would occur. There are no specific design limits associated with cladding rupture other than that the degree of swelling will not be underestimated and the ballooning will not block the coolant channel Additionally, the time of rupture needs to be known so that oxidation on the cladding inner surface and its associated heat is correctly modeled.

An applicant will typically use an empirical correlation for burst stress and ballooning strain such as the one given in NUREG-0630 (Powers and Meyer 1980); however, NUREG-0630 was developed for Zr-based alloys. If an applicant uses NUREG-0630 for FeCrAl cladding, burst criteria would first need to be established, followed by collecting data to show that the performance of FeCrAl is bounded by these limits. Alternatively, if the applicant wants to propose new burst stress and ballooning strain limits, a significant body of burst data would be useful to show that the degree of swelling will not be underestimated.

Currently available data suggest that for FeCrAl cladding, the increased oxidation resistance minimizes or eliminates the occurrence of ballooning and burst of cladding (Rebak, Terrani, and Fawcett 2016; Massey et al. 2016). The lack of diametrical strain, coupled with notably larger burst openings for ferritic Fe-based alloys implies that ballooning was minimal prior to burst and the majority of deformation occurred once the onset of mechanical instability had been reached and rapid plastic deformation had taken place locally at the burst opening (Massey et al. 2016).

Testing: Ballooning and Bursting

Table 4-6 summarizes the ballooning tests that have been conducted for FeCrAl alloys. Massey et al.suggested that minor compositional changes between FeCrAl alloys does not affect burst behavior; however as the two FeCrAl alloys tested in that study would fall into two different areas of Figure 3-2 (Fe-13Cr-5Al in 'compositions with no known issues' and Fe-15Cr-4Al in 'α' embrittlement'), it is recommended that further testing is completed to determine if there is a compositional dependence for ballooning and burst behavior.

Table 4-6. Summary of ballooning data for FeCrAl cladding.

Lead	FeCrAl Alloy(s)s	Test Description	Results
ORNL (Massey et al. 2016)	Fe-13Cr-5Al Fe-15Cr-4Al	Burst tests in steam, internally pressurized with He	FeCrAl alloys demonstrated ~10% higher temperature at the onset of burst in comparison to Zr-based alloys FeCrAl alloys exhibited significantly smaller diametrical strains in comparison with Zr-based alloys Minor compositional changes between FeCrAl alloys did not affect burst behavior
ORNL (Kane et al. 2020)	C26M	Simulated cyclic dryout test; internally pressurized and subjected to rapid 300-650 °C, 300-700 °C, and 300-800 °C thermal cycling in steam environment	C26M remained virtually undeformed after completing 54 cycles between 300-650 °C Burst after 20 cycles between 300-700 °C Burst during the first cycle between 300-800 °C
North Carolina State University (Joshi et al. 2020)	C26M2	Burst tests, internally pressurized with argon, in the temperature range of 753-923 K	Cladding tubes failed with very little or no ballooning Steady-state creep rate

4.3.2.4 High-Temperature Oxidation

The oxides developed in FeCrAl alloys (chromia and alumina) differ from the zirconium oxide developed in Zr-based alloys. Under normal operating conditions, FeCrAl alloys are protected by a thin layer of oxide rich in chromium. As the temperature increases, a thin layer of alumina develops underneath the chromia; the alumina develops rapidly between 800 °C and 950 °C (Berthomé et al. 2005). Beyond 1100 °C, the chromia evaporates, typically leaving behind the thin alumina layer, which protects the FeCrAl up to its melting point (Rebak 2018a).

Figure 4-7, reproduced from (Schuster, Crawford, and Rebak 2017), shows the generalized oxidation behavior of FeCrAl alloys in the presence of steam.

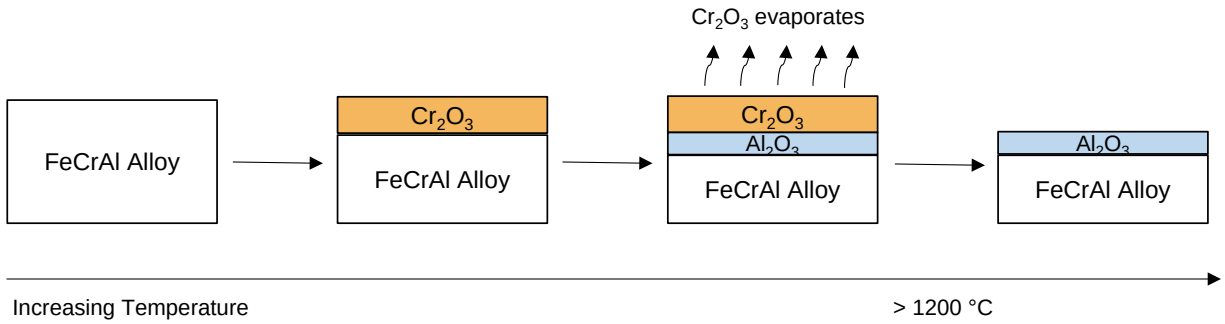

Figure 4-7. Oxidation behavior of FeCrAl alloys in presence of steam (Schuster, Crawford, and Rebak 2017).

However, it has been observed that at a certain temperature (1400 °C for Tang et al.) the alumina layer is no longer protective, resulting in catastrophic oxidation. Additionally, it has been suggested that lower-Cr content FeCrAl alloys need an Al content ≥ 5% to form an alumina layer (Pint et al. 2015). Further study on the composition dependence of oxide formation (both oxide composition and transition temperatures) is needed.

Kanthal APMT tubes are available pre-oxidized (i.e., with an alumina layer on the surface) (Kanthal 2019).

Recent analysis of the QUENCH-19 test suggests that oxidation kinetics derived from temperatures above the chromia evaporation point may not accurately capture behavior at lower temperatures (Stuckert et al. 2019); further study is needed as all tests summarized in Table 4-7 took place at or above 1200 °C.

Limit: Cladding Oxidation, Hydriding, and CRUD

For Zr-based alloy cladding, the cladding oxidation limit is designed to preclude oxide spallation that has typically been observed above 100 µm. Oxide spallation can lead to a local cool spot which acts as a sink for hydrides, creating a local, extremely brittle hydride lens, designated as CRUD. The hydrogen limit is designed to ensure the strain limit previously identified will be applicable since high levels of hydrogen (>600 ppm) can cause embrittlement of the cladding. Hydrogen is not the only embrittlement mechanism and there may be other embrittlement mechanisms that are discussed elsewhere. There is no explicit limit on CRUD, other than it be considered if it is present. It is typically modeled as an insulating layer around the fuel rod in plants that have CRUD issues.

Limits should be proposed that preclude environmental damage to the protective chromia and alumina layers and subsequent embrittlement of the cladding. CRUD should be monitored in plants and be explicitly considered and modeled as an insulating layer around the fuel rod if it is present.

Testing: High-Temperature Oxidation

Table 4-7 summarizes the high-temperature oxidation testing for FeCrAl cladding. Further study is recommended to determine composition dependence on steam oxidation resistance; additionally, tests should be conducted at lower temperatures than previously studied to determine if oxidation kinetics at temperatures lower than the chromia evaporation point are properly represented with existing data.

Table 4-7. Summary of high-temperature oxidation data for FeCrAl cladding.

Lead	FeCrAl Alloy(s)s	Test Description	Results
ORNL (Pint et al. 2015)	Fe-15Cr-5Al-Y Fe-13Cr-5Al-Y C135 C135C C135Nb Kanthal APMT MA956 Kanthal APM SUH21 Alkrothal 720 Alkrothal 14 Alkrothal 3 Ohmaloy30 Ohmaloy40	Oxidation experiments in three different systems: 1) 1 bar of Ar-50% H_2O or dry air at 1200 °C 2) Dry air or 100% steam at 800 °C to 1500 °C 3) Pre-heated to 1000 °C to 1300 °C	Lower-Cr content alloys require Al content ≥5% to form an alumina layer There is an apparent composition dependence on steam oxidation resistance
GE Global Research (Rebak, Jurewicz, and Y.-J. Kim 2017)	Kanthal APMT	Pre-exposed to high-temperature water for 73 days then exposed to 1200 °C steam	Alumina layer forms in steam on specimens previously exposed to high-temperature water; alumina layer of pre-oxidized FeCrAl dissolved when exposed to high-temperature water and acts like non-pre-oxidized FeCrAl
GE Global Research (Schuster, Crawford, and Rebak 2017)	Kanthal APMT	1200 °C in 100% steam for 4 h and then quenched in water	High resistance to oxidation by formation of alumina layer, which remained adherent to the surface after quenching

Lead	FeCrAl Alloy(s)s	Test Description	Results
Karlsruhe Institute of Technology (Tang et al. 2018)	Fe-6Cr-6Al Fe-8Cr-6Al Fe-10Cr-5Al Fe-14Cr-4Al Fe-15Cr-4Al Fe-6Cr-8Al Fe-10Cr-7Al Fe-12Cr-7Al Fe-16Cr-6Al Fe-12Cr-5Al Fe-12Cr-8Al Fe-16Cr-8Al Fe-12Cr-5Al-0.3Y Fe-16Cr-8Al-0.3Y Kanthal APM Kanthal D	Steam/argon between 1200 and 1500 °C for 1 h or 15 min	Increasing Al and Cr contents and decreasing heating ramp rate improved the alloy's resistance to steam in transient tests Isothermal oxidation at 1200 °C and 1300 °C resulted in catastrophic oxidation of alloys with low Cr and Al content All samples experienced catastrophic oxidation at 1400 °C Protective oxide layer demonstrated at 1500 °C
Pusan National University (S. Kim, Moon, and Bahn 2019)	Fe-13Cr-6Al Fe-13Cr-6Al-0.15Y Fe-13Cr-6Al-0.3Y Fe-13Cr-6Al-0.45Y	1200 °C steam/Ar for 10 min, 3 h, and 24 h	Yttrium addition enhances oxidation resistance
Karlsruhe Institute of Technology (Stuckert et al. 2019)	Kanthal APM B136Y3	Pre-oxidation, heat-up, extended period (constant electrical power), quench (water flow rate 48 g/s)	Measured peak cladding temperature 1455 °C Coping time approximately 3200 s (compared to 1200 s for a similar test with Zr-based alloys) though using this to assess for reactor conditions should be made with care Cladding damaged by 1) probable melting or by interaction with molten thermocouples or 2) parts of claddings were spalled Total hydrogen production higher than code predictions; correlations may be incorrect at temperatures between 1300 °C and 1500 °C

4.3.2.5 Fretting

Current design limits state that fuel rod failures will not occur due to fretting, which has historically been controlled through debris filters (reducing the possibility of debris fretting) and through spacer design (reducing fretting between fuel rods and grid features). The increased elastic modulus of FeCrAl compared to Zr-based alloys reduces fretting amplitude and improves fretting wear but fretting in LWR-representative water conditions should be evaluated to demonstrate that FeCrAl will not be damaged by assembly grids and vice versa.

Zr-based grids could be more susceptible to grid-to-rod fretting compared to a high-Cr FeCrAl-based grid when FeCrAl-based rods are used within a fuel assembly. Additional studies are needed to evaluate the fretting and wear characteristics of lower-Cr FeCrAl alloys.

Table 4-8. Summary of unirradiated fretting and wear testing for FeCrAl alloys.

Lead	FeCrAl Alloy(s)s	Test Description	Results
KAERI (Y.-H. Lee and Byun 2015)	Fe-21Cr-5Al	Reciprocating sliding testing in room temperature air and water	Wear depth with water lubrication was strongly dependent on the bulk hardness; no severe plastic deformation; wear decreased by nearly an order of magnitude in water lubrication
Georgia Institute of Technology (Winter et al. 2018)	Kanthal APMT	DN55 fretting machine in dry PWR conditions	Favorable wear in dry PWR conditions compared to Zircaloy-4

4.3.2.6 Thermal Limits

Limit: Overheating of Cladding

Overheating of the cladding refers to exceeding critical heat flux (CHF) and is applicable to AOOs and some accident analyses. Operation above this point results in a reduction of the coolant's ability to remove heat and can result in cladding damage. In a PWR, exceeding CHF results in DNB; in a BWR, exceeding CHF results in dryout. This thermal margin should not be exceeded for normal operation and AOOs. For DBAs, the number of fuel rods exceeding thermal margin criteria are assumed to have failed and are included in fission product release dose calculations.

The boiling transitions are shown in Figure 4-8. Typical limits are based on ex-reactor flow tests on electrically heated fuel assembly mockups to determine where CHF occurs. CHF is primarily influenced by the geometry of the assembly, although surface conditions (including surface roughness, wettability, and porosity) of the fuel rods may also have an impact. Most studies have concluded that roughness has little to no impact on CHF (Collier and Thome 1994; Kandlikar 2001; O'Hanley et al. 2013) though some studies have shown a noticeable difference between rough and very smooth surfaces (Weatherford 1963). Surface porosity and wettability are thought to have a much more significant impact, as demonstrated by several experimental studies (Kandlikar 2001; Takata et al. 2003; O'Hanley et al. 2013).

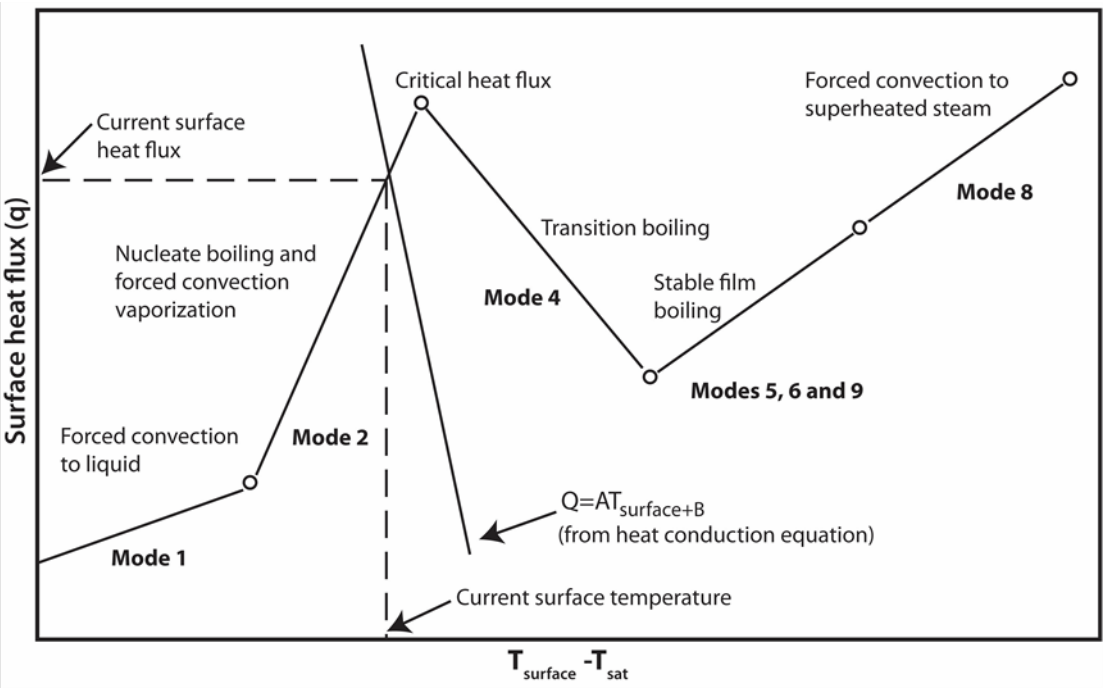

Figure 4-8. Typical boiling transitions.

Corrosion studies indicate higher surface roughness and wettability values and lower contact angles for FeCrAl samples compared to Zircaloy-4 in typical LWR environments (Terrani et al. 2016). Pool boiling experiments indicate that the presence of the oxide layer on a FeCrAl sample increases the measured CHF compared to as-machined samples; as-machined samples were found to have a higher heat transfer coefficient than oxidized samples (Ali et al. 2018).

Ex-reactor flow tests on electrically heated fuel assembly mockups could be performed to determine where CHF occurs. Currently, many CHF tests are performed on Inconel assemblies;

this may not provide a faithful representation of FeCrAl CHF characteristics. Use of Inconel in CHF testing should be justified as conservative or appropriate for determining FeCrAl CHF behavior.

Pool boiling CHF does not directly translate to flow boiling CHF but provide a first estimate of the performance of FeCrAl under AOO and some accident conditions. The study by Lee (S. K. Lee et al. 2019) suggests that the effect of surface properties on the flow boiling CHF is limited in tested flow conditions and recommends revisiting current CHF correlations and lookup tables, all of which were developed with steel-based materials. However, if it is possible to demonstrate existing correlations provide conservative CHF predictions for FeCrAl alloy cladding, existing correlations may be appropriate. Further testing is recommended.

Testing: Thermal Limits

Table 4-9 summarizes the testing done on the unirradiated thermal limits for FeCrAl cladding.

Table 4-9. Summary of unirradiated thermal limit testing for FeCrAl cladding.

Lead	FeCrAl Alloy(s)s	Test Description	Results
University of New Mexico (S. K. Lee et al. 2019)	Fe-13Cr-6Al	Repeated steady-state and transient internal-flow CHF experiments under atmospheric pressure, a fixed inlet temperature (40 or 60 °C) and mass flow of 300 kg/m^2-s	Despite notable changes of wettability, roughness, and oxide layer characteristics on samples that had already been subjected to CHF testing, measured flow CHF remained unchanged throughout repeated experiments for tested materials Material properties considered primarily responsible for the observed CHF differences among tested materials; suggest revisiting current CHF correlations and lookup tables (developed with steel-based materials)

4.3.2.7 LOCA Post-Quench Ductility

There are no extensive studies on the LOCA post-quench ductility of FeCrAl cladding. However, it is expected that FeCrAl will behave favorably to Zr-based alloys, retaining mechanical properties post-quench. Further testing is recommended to determine if this is true for all FeCrAl alloys, including Kanthal APMT and MA956, which have been noted to show α' embrittlement per Figure 3-2 . Similar to SS-304 and other metallic alloys, ductility is expected to decrease with irradiation (Rebak, Terrani, and Fawcett 2016)

Table 4-10. Summary of LOCA post-quench ductility for unirradiated FeCrAl cladding.

Lead	FeCrAl Alloy(s)s	Test Description	Results
GE Global Research (Dolley et al. 2018)	Kanthal APMT	Exposed to steam, argon, and air at 1200 °C for 2 h before rapid quenching in water; post-quench tensile tests	APMT showed consistent mechanical behavior in each condition tested, showing lower strain-to-failure than other tested alloys (including Zircaloy-2)

4.3.2.8 Other Data

This section discusses other related data, including weld qualification, materials interactions, and autoclave testing.

Testing: Weld Qualification Data

Austenitic stainless steels experienced weld-associated cracking from the coolant side when used before as fuel cladding. Ferritic alloys are highly resistant to SCC and a study has shown that IronClad alloys did not experience weld sensitization or other phase transformation, as summarized in Table 4-11.

Table 4-11. Summary of weld qualification data for FeCrAl cladding.

Lead	FeCrAl Alloy(s)s	Test Description	Results
GE Global Research (Rebak et al. 2018b)	Kanthal APMT C26M	Heat treated at 677 °C for 2 h and 732 °C for 1 h TIG welding	Welded joints found to be fully hermetic and free from cracks, oxidation, and porosity

Testing: Materials Interactions

The interactions of FeCrAl with various materials found in-reactor have been studied for any possible material interactions and are summarized in Table 4-12. FeCrAl alloys have shown excellent resistance to materials interaction compared to Zr-based alloys but further testing is recommended to determine if there is any composition dependence.

Table 4-12. Summary of unirradiated materials interactions for FeCrAl cladding.

Lead	FeCrAl Alloy(s)s	Test Description	Results
Nippon Nuclear Fuel Development (Sakamoto et al. 2016)	Fe-12Cr-6Al-ODS	FeCrAl/UO_2 and FeCrAl/B_4C couples in argon gas at 1573 K and 1673 K	No distinct reaction between FeCrAl/UO_2 couple with a uniform alumina layer and no clear ingress of uranium FeCrAl/B_4C showed excellent resistance to interaction
ORNL (Robb, Howell, and Ott 2018)	Fe-13Cr-6.2Al-0.3Y	FeCrAl/Inconel, and FeCrAl/B_4C couples in a furnace at temperatures ranging from 1300 °C to 1450 °C FeCrAl/SS-304H couples in a furnace at temperatures ranging from 1300 °C to 1400 °C	No signs of interaction

While not included in Table 4-12, the QUENCH-19 results saw potential interactions between FeCrAl (Alloy B136Y) and SS-304 thermocouples (Stuckert et al. 2019). This could indicate eutectic interaction between FeCrAl and SS-304; however, it is possible that the cladding reached the melting point of FeCrAl as there were uncertainties in the temperature measurements and several thermocouples failed. See Section 3.5 for more details.

Testing: Autoclave

Autoclave tests are useful for screening new materials and indicating if one material will have improved corrosion resistance relative to another; however, in-reactor corrosion rates should not be deduced from autoclave test data. These rates should be obtained from in-reactor measurements from fueled rods at typical power levels in prototypical coolant conditions.

Table 4-13. Summary of autoclave data for unirradiated FeCrAl cladding.

Lead	FeCrAl Alloy(s)s	Test Description	Results
ORNL (Terrani et al. 2016)	Fe18Cr3Al Fe15Cr4Al Fe13Cr4Al-SG Fe13Cr4Al Fe12Cr5Al Fe10Cr5Al	3.57 ppm H_2, 330 °C, pH 7.2, 15 MPa 0.3 ppm H_2, 290 °C, pH 5.6, 7 MPa 1.0 ppm O_2, 290 °C, pH 5.6, 7 MPa	Parabolic oxidation and dissolution rates Maximum thickness loss after one year ~2µm
GE Global Research (Rebak, Jurewicz, and Y.-J. Kim 2017)	Kanthal APMT	330 °C, 3.75 ppm H_2 290 °C, 0.3 ppm H_2 290 °C, 1 ppm O_2	Corrosion resistant in high-temperature hydrogenated and oxygenated water
The University of New Mexico (Ali et al. 2018)	Fe12Cr5Al Fe13Cr4Al	3.57 ppm H_2, 330 °C, pH 7.2, 15 MPa 0.3 ppm H_2, 290 °C, pH 5.6, 7 MPa 1.0 ppm O_2, 290 °C, pH 5.6, 7 MPa	Surface roughness, contact angles, oxide layer thickness, CHF and DNBR predictions
Ulsan National Institute of Science and Technology (T. Kim et al. 2019)	Fe14Cr4Al Fe14Cr4Al-Y Fe13Cr6Al-0.15Y	360 °C, 20 MPa, 100-1200 ppm boron, pH near 7	FeCrAl with higher Al contents show higher corrosion resistance; yttrium addition has a beneficial effect on corrosion resistance
GE Global Research (Rebak et al. 2019)	Kanthal APMT C26M FeCrAl-ODS	330 °C, 3.75 ppm H_2 288 °C, 0.3 ppm H_2 288 °C, 1 ppm O_2	FeCrAl experienced mass loss; largest amount of mass loss was for C26M and FeCrAl-ODS (both with 12% Cr) in hydrogenated waters
ORNL (Raiman et al. 2020)	Fe-10Cr-6Al-2Mo Fe-13Cr-5Al-2Mo Fe-13Cr-5Al-2Mo Fe-13Cr-6Al-2Mo Fe-13Cr-7Al-2Mo Fe-13Cr-5Al-2Mo-1Nb Kanthal APMT	BWR normal water chemistry and BWR hydrogen water chemistry	A representative mass loss of approximately 60 µm over 6 years

4.3.3 Ex-Reactor Data Collected on Irradiated Samples

Recommended qualification data from ex-reactor tests on irradiated samples are:

1. Elastic modulus
2. Yield stress
3. Uniform elongation/ductility (normal operation and AOO)
4. Uniform elongation/ductility (RIA)
5. Fatigue.

The following will describe the data and overall observations that are available.

4.3.3.1 Mechanical Properties

Limit: Irradiation Growth

The assembly design allows for a given amount of growth and will define the limit for irradiation growth. The axial growth below will be used to assess maximum growth. Assessments must be done to determine axial irradiation growth of FeCrAl cladding. Additionally, irradiation creep data for FeCrAl is only available at low doses (<1 dpa) (Field 2018); further high-dose data is needed.

Limit: Mechanical Fracturing

Mechanical fracturing refers to a defect in the cladding caused by an externally applied force. Typically, this limit has conservatively been set as applied stressed about 90% of the irradiated yield stress. This limit should not be exceeded for normal operation and AOOs. For DBAs, the number of fuel rods exceeding this limit are assumed to have failed and are included in fission product release dose calculations. This limit is acceptable for FeCrAl cladding given that the irradiated yield stress obtained as described below is used.

Limit: Excessive Fuel Enthalpy

Excessive fuel enthalpy relates to the sudden increase in fuel enthalpy from an RIA below the fuel melting limit which can result in cladding failure due to PCMI. Current fuel enthalpy limits are based on RIA tests that have been performed on irradiated and unirradiated fuel rodlets in various test reactors and a limit of what level of fuel enthalpy increase will cause cladding failure has been determined.

For Zr-based alloy cladding, these data have been collected over a very long period of time and it may not be practical to collect this amount of data for FeCrAl cladding.

An alternate approach comes from the fact that cladding failure due to excessive fuel enthalpy is driven by PCMI, which causes the cladding to exceed its ductility limit. It is possible to collect uniform elongation (strain at maximum load) data from the irradiated cladding mechanical tests that need to be performed to collect the elastic modulus and yield stress data. If it can be shown that FeCrAl cladding has a beneficial or negligible impact on the uniform elongation relative to the reference Zr-based alloy cladding, it could be reasonably argued that the current RIA failure limits are applicable to FeCrAl cladding; a more limited number of RIA tests on FeCrAl-clad fuel rods or a commitment to collecting such data may be acceptable.

It should be noted that the current limits are written in terms of enthalpy deposition caused by the RIA; it must be shown that these limits remain applicable to larger fuel pellets and thinner cladding. Additionally, this limit is used to assess the number of fuel rods that are expected to fail during an RIA and a conservative approach could be taken to either assume all the rods will fail or a significantly conservative limit could be applied to cover the lack of RIA test data on FeCrAl cladding.

Limit: Structural Deformation

Structural deformation refers to externally applied loads during a LOCA or safe shutdown earthquake that could deform the fuel assemblies or cause fuel fragmentation such that coolable geometry would be lost. This limit has conservatively been set as applied stresses above 90% of the irradiated yield stress. For DBAs, the number of fuel rods exceeding this limit are assumed to have failed and are included in fission product release dose calculations. This limit is acceptable for FeCrAl cladding given that the irradiated yield stress obtained as described below is used.

Testing: Mechanical Properties

Mechanical properties of irradiated FeCrAl cladding have been studied and are summarized in Table 4-14. Irradiated rods should be investigated further as irradiation hardens the cladding and leads to significant increase in the yield stress and ultimate tensile strength. Fueled rods are preferable, as the in-reactor temperature and heat flux across the cladding can impact the competing creation and annealing of lattice defects that lead to this hardening and this temperature may be different for fueled and unfueled rods.

Table 4-14. Summary of mechanical property testing for irradiated FeCrAl cladding.

Lead	FeCrAl Alloy(s)s	Test Description	Results
ORNL (Field et al. 2015)	Fe-10Cr-4.8Al Fe-12Cr-4.4Al Fe-15Cr-3.9Al Fe-18Cr-2.9Al	Tensile tests at room temperature (only one test per sample)	Room temperature engineering stress-strain curves
ORNL (Field et al. 2017)	F1C5AY Kanthal APMT	Tensile tests at room temperature and 320 °C	Stress-strain curve, tensile response as a function of dose, 0.2% offset yield strength, ultimate tensile strength, uniform elongation, total elongation
ORNL (Chen et al. 2019)	C06M C36M	Vickers microhardness testing with 1 kg force and 15 s dwell time Transition fracture toughness testing	Master Curve transition temperature; reasonable linear correlation between the Master Curve fracture toughness transition temperature and Vickers microhardness
University of New Mexico (Z. Zhang et al. 2020)	MA956	Tensile tests at room temperature	Yield stress, ultimate tensile strength, uniform elongation, total elongation; hardening and ductility reduction after irradiation were observed

The following sections compare the irradiated mechanical properties of FeCrAl alloys (C26M, Kanthal APMT, MA956, and/or a generalized correlation where applicable) to the irradiated mechanical properties of Zr-based alloys.

Material Property: Irradiated Yield Stress

Figure 4-9 shows the 320 °C yield stress for Kanthal APMT after neutron irradiation (Field et al. 2017).

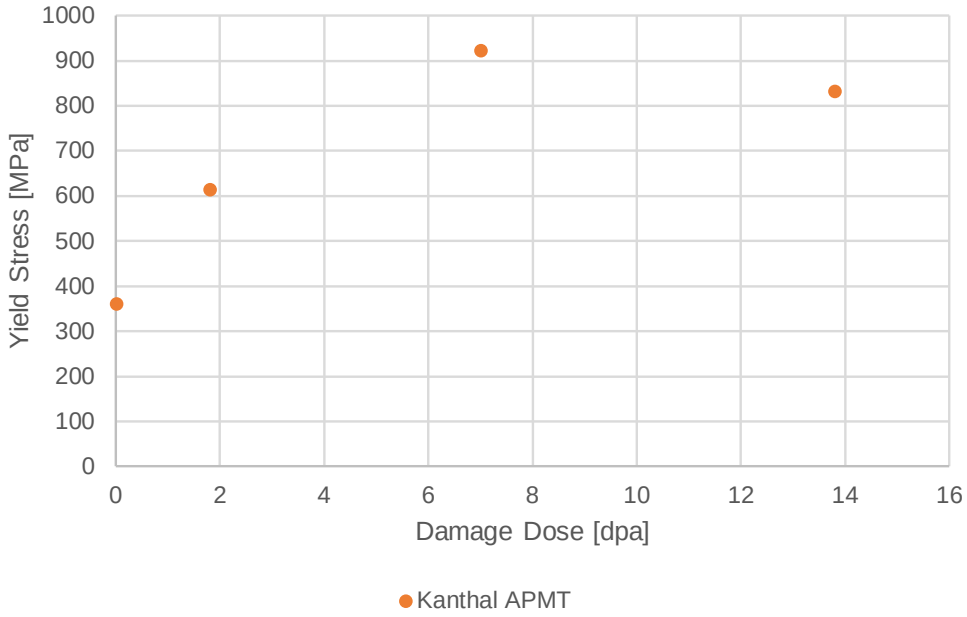

Figure 4-9. Irradiated yield stress for Kanthal APMT at 320 °C (Field et al. 2017).

The yield stress of Kanthal APMT increases up to ~7 displacements per atom (dpa) and then saturation of the hardening occurs above this dose. Lower Cr-content variants of FeCrAl are less susceptible to brittle fracture above 7 dpa when irradiated at near LWR-relevant temperatures. Lower-Cr content variants maintain adequate mechanical performance in the context of tensile properties after neutron irradiation for ATF LWR cladding applications when compared to Zr-based alloys (Field et al. 2017).

Material Property: Axial Irradiation Growth

There is a lack of measured axial irradiation growth data for the various FeCrAl alloys. Figure 4-10 shows the correlations used in MatLib to model the axial irradiation growth of FeCrAl and Zr-based alloys (Geelhood et al. 2020).

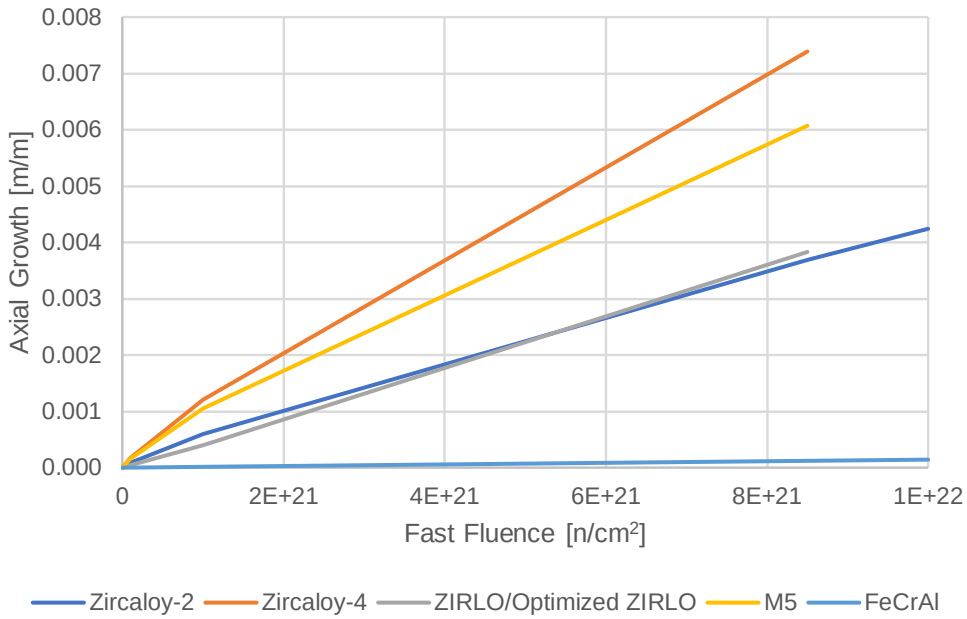

Figure 4-10. MatLib correlations for axial irradiation growth of Zr-based alloys and FeCrAl alloys (Geelhood et al. 2020).

4.3.3.2 Fatigue

Limit: Cladding Fatigue

The cladding fatigue limit is typically based on the sum of the damage fractions from all the expected strain events being less than 1.0. The damage fractions are usually found relative to the O'Donnell and Langer irradiated fatigue design curve (O'Donnell and Langer 1964). It is currently unknown if this curve applies to FeCrAl tubes. Limited tests have been done on the fatigue properties of FeCrAl and there is an indication that there is a potential composition dependency (Field 2018). The existing fatigue data is for unirradiated FeCrAl; it is summarized in Table 4-15.

Fatigue data from irradiated cladding, produced using a representative process for the applicant in question, is recommended to either confirm the O'Donnell and Langer irradiated fatigue design curve applies or develop a new curve. New fatigue design curves should include a safety factor of two on stress amplitude or a safety factor of 20 on the number of cycles as mentioned in NUREG-0800 Section 4.2 (U.S. NRC 2007).

Testing: Fatigue

Table 4-15. Summary of fatigue data for unirradiated FeCrAl cladding.

Lead	FeCrAl Alloy(s)s	Test Description	Results
City University of Hong Kong (Field 2018)	Fe-23.85Cr-3.89Al De-25Cr-2Al	Various strain amplitudes at various temperatures	Three-stage behavior: 1) hardening, 2) saturation, and 3) softening followed by fracture, showing a dependence on temperature and strain amplitude Indicated a potential composition dependency

4.3.3.3 Other Data

This section discusses other related reactor data.

Weld Qualification Data

Tensile tests have been performed on irradiated and nonirradiated welds. Low- to mid-temperature neutron irradiation revealed strong embrittlement of the welds but high-temperature neutron irradiation had little effect on the properties, suggesting that a ductile-to-brittle transition occurs at ~380 °C to 400 °C.

Table 4-16. Summary of irradiated weld qualification data for FeCrAl cladding.

Lead	FeCrAl Alloy(s)s	Test Description	Results
ORNL (Gussev, Cakmak, and Field 2018)	C35M C37M C35M10TC	Tensile tests of welded, irradiated and nonirradiated samples	Low-temperature neutron irradiation led to strong embrittlement of the weldments Mid-temperature neutron irradiation revealed strong embrittlement for C37M and C35M10TC High-temperature neutron irradiation had little effect on the properties, suggesting that a ductile-to-brittle transition occurs at ~380 to 400 °C

4.4 Additional SAFDLs and Recommended Testing

This section recommends additional testing needed to support developing and justifying limits and summarizes any remaining SAFDLs not covered in the previous sections.

4.4.1 SAFDLs: Assembly Performance

SAFDLs related to assembly performance are typically performed by simple hand calculations or by citing manufacturing controls or historic data. These limits may need a revision relative to those typically used for Zr-based alloy tubes.

4.4.1.1 Rod Bow

Typically, there is a penalty on departure from nucleate boiling ratio (DNBR) or margin to critical power ratio (MCPR) to account for bowing. The limit on the acceptable degree of bowing will not change with the use of FeCrAl cladding as it is controlled by the physical dimensions of the fuel assembly. However, as FeCrAl-clad fuel rods will likely have a thinner wall thickness (due to higher neutron absorption), testing or assessments of LTAs should be done to show rod bow is not a concern.

4.4.1.2 Hydraulic Lift Loads

The limits for hydraulic lift loads are such that the upward hydraulic forces do not exceed the weight of the assembly and the downward force of the holddown springs. None of these parameters are expected to change with the introduction of FeCrAl cladding; existing limits and methods are expected to be adequate.

4.4.1.3 Fuel Assembly Lateral Deflections

The limits for fuel assembly lateral deflections are such that control rods (in a PWR) or control blades (in a BWR) can still be inserted as needed. Current assembly and channel bow methods are used to assess performance relative to these limits. Assembly and channel bow are not impacted by fuel rod performance, but rather by guide tube design (in a PWR) and channel design (in a BWR) and, therefore, these limits and methods are not expected to change with the introduction of FeCrAl cladding.

4.4.2 SAFDLs: Fuel Rod Performance (Normal Operation and AOO)

Current codes informed by material properties can perform the analyses required in this subsection. However, the limits may need revision relative to those typically used for Zr-based alloy tubes. Several of these SAFDLs also have application in accident analysis.

4.4.2.1 Internal Hydriding

Internal hydriding is typically addressed through manufacturing controls on the pellet moisture limit. Hydrogen does not chemically accumulate in FeCrAl alloys (Rebak, Terrani, and Fawcett 2016).

4.4.2.2 Overheating of Fuel Pellets

For this analysis, the limit is the melting temperature of the fuel pellets. This will not be impacted by the introduction of FeCrAl cladding and the limit for this SAFDL may stay the same.

4.4.2.3 Pellet-to-Cladding Interaction

Typically, there is no explicit limit set on pellet-to-cladding interaction. Various manufacturing designs and inspections and the transient cladding strain limit are expected to cover this SAFDL. No eutectics between FeCrAl and UO_2 or fission products have been identified (see Section 3.5).

4.4.3 SAFDLs: Fuel Rod Performance (Accident Conditions)

Current codes informed by material properties can perform the analyses required in this subsection. However, the limits may need revision relative to those typically used for Zr-based alloy tubes. Several of these SAFDLs also have application in AOO analysis.

Work is underway to change some regulations (10 CFR 50.46c) and staff guidance (DG-1327) for LOCA and RIA analysis. Neither of these is compete yet, so the discussion in this report will reflect the current regulations and staff guidance.

4.4.3.1 Cladding Embrittlement

Cladding embrittlement related to embrittlement of the fuel cladding, particularly in the ballooned region of the cladding during LOCA. Cladding embrittlement during LOCA should be precluded so the fuel assemblies with ballooned rods are not severely damaged by post-LOCA loads such as reflood and quenching, including blowdown loads. 10 CFR 50.46 specifies a cladding temperature limit of 2200 °F (1204 °C) and a peak oxidation of 17% equivalent cladding reacted (ECR) for Zr-based alloy cladding (U.S. NRC 2017).

As FeCrAl does not oxidize to the extent a Zr-based alloy does, the 17% ECR is not applicable. However, significant irradiation embrittlement was observed for both C06M and C36M (Chen et al. 2019). Tests showing ductility (see Section 4.3.2.7) at either these existing limits or tests establishing new limits would be useful to demonstrate embrittlement will not occur. In addition to the tests performed to establish the ballooning (Section 4.3.2.3) and high-temperature oxidation (Section 4.3.2.4) behavior, some prototypic integral LOCA tests where cladding tubes are subjected to ballooning and burst in steam under expected time frames and subsequent samples are subjected to mechanical loading (such as bend tests) after ballooning, burst, and high-temperature oxidation are very useful to establish cladding embrittlement limits. For these tests, irradiated cladding tubes are preferable.

4.4.3.2 Violent Expulsion of Fuel

Violent expulsion of fuel relates to the sudden increase in fuel enthalpy from an RIA that can result in melting, fragmentation, and dispersal of fuel. This could result in a loss of coolable geometry and produce a pressure pulse that could damage the reactor vessel. Typical limits for violent expulsion of fuel are:

- Peak radial average fuel enthalpy below 230 cal/g;
- Peak fuel temperature below the melting point.

It is expected that cladding failure will occur well before 230 cal/g for both Zr-based alloy cladding and FeCrAl cladding due to excessive fuel enthalpy (see Section 4.3.3.1). The limit on violent expulsion of fuel is derived to prevent rapid ejection of fuel from failed cladding. As such, this limit relates more to the fuel than to the cladding and are expected to be appropriate for FeCrAl cladding.

4.4.3.3 Generalized Cladding Melting

Generalized cladding melting is applicable to DBAs and is set to preclude the loss of coolable geometry. The limit is set as the cladding melting temperature, which for Zr is 1852 °C. For Zr-based alloy tubes, the embrittlement limit of 1204 °C (see Section 4.4.3.1) is more limiting. The typical melting temperature of FeCrAl is 1500 °C, though this may vary slightly based on final alloy composition (Field 2018). However, as discussed above, it is unknown what the limit for FeCrAl embrittlement will be, so cladding melting should still be considered for FeCrAl.

4.5 Changes to Existing Codes and Methodologies

This section describes the changes to the existing codes and methodologies, including the need for validation.

4.5.1 Codes

While material property updates must be made to codes, the critical need for the updated codes is validation, which is typically performed on five areas that directly relate to various SAFDLs. These are also the areas used to assess FAST (Porter et al. 2020).

1. Fuel temperature
2. Fission gas release
3. Rod internal pressure and internal void volume
4. Cladding oxide thickness
5. Cladding permanent hoop strain following a power ramp.

If it is determined that FeCrAl has an impact on the CHF correlations, then testing should also be performed to determine the CHF correlation for FeCrAl cladding for subchannel or systems analysis codes. Table 4-17 provides recommended tests for use in code assessment.

Table 4-17. Assessment data for validation of fuel thermal-mechanical codes for FeCrAl alloy tubes and recommended tests for data collection.

Assessment Data	Recommended Tests
Fuel centerline temperature	Any that can be obtained; not critical
Fission gas release	LTA data and ongoing surveillance plan
Rod internal pressure and void volume	LTA data and ongoing surveillance plan
Cladding oxide thickness	Initially none beyond data in Table 4-7 and ongoing surveillance plan
Cladding permanent hoop strain following a power ramp	Power ramp tests to assess the prediction of cladding strain following power ramp

4.5.1.1 Fuel Temperature

A fuel thermal-mechanical code will be used to assess the power-to-melt limit as well as provide initial conditions to accident analyses. FeCrAl-clad UO_2 is expected to utilize larger diameter fuel pellets; this will cause the thermal gradients across the fuel to be steeper. Previous simulations comparing to a Zr-based/UO_2 system found the maximum fuel temperature difference to be approximately 50 K.

Historically, temperature data was collected in the Halden Reactor, now permanently shut down; the ATF-2 campaign at the ATR, currently ongoing, includes instrumentation for measuring fuel centerline temperature. However, given that the cladding properties are correctly implemented into a fuel thermal-mechanical code, it is reasonable to assume that fuel temperatures will be correctly predicted.

4.5.1.2 Fission Gas Release

Fission gas release is primarily driven by fuel temperature, time, and power level. Fission gas release can drive fuel temperatures and rod internal pressure and as such is a key metric of success in a fuel thermal-mechanical code. As mentioned above, a validated fuel code should adequately predict the fuel temperature, so the fission gas release should also be adequately predicted.

Any fission gas released from destructive examination of LTAs, particularly high-power LTAs, would be useful in the assessment of a thermal-mechanical code used for safety analysis of FeCrAl cladding. An ongoing surveillance plan with the goal of continuing to obtain more fission gas release data would provide additional assessment data.

4.5.1.3 Rod Internal Pressure and Internal Void Volume

A fuel thermal-mechanical code will be used to assess the rod internal pressure relative to the pressure limit, derived by the applicant. Void volume is impacted by component temperatures and deformations and could be impacted if the FeCrAl cladding has a significantly different creep rate than Zr-based alloy cladding. Rod internal pressure is driven primarily by void volume. Fission gas release and component temperature and could also be impacted.

Any void volume or rod internal pressure data from destructive examination of LTAs, particularly high-power LTAs, would be useful in the assessment of a thermal-mechanical code used for safety analysis of FeCrAl cladding. An ongoing surveillance plan with the goal of continuing to obtain more void volume and rod internal pressure data would provide additional assessment data.

4.5.1.4 Cladding Oxide Thickness

Cladding oxide thickness can have a feedback on the fuel and cladding temperature predictions. A fuel performance code will be used to assess the cladding oxide thickness relative to limits derived by the applicant. However, the cladding oxide thickness of FeCrAl cladding is very small and probably does not need to be accounted for.

4.5.1.5 Cladding Permanent Hoop Strain Following a Power Ramp

A fuel thermal-mechanical code will be used to assess the cladding permanent hoop strain during an AOO power ramp and compare to the cladding strain limit. Power ramp tests on rodlets refabricated from irradiated fuel rods would be helpful to assess the code prediction of hoop strain following a power ramp. If it can be demonstrated that the impact of FeCrAl cladding is minimal or can be accounted for with the code and associated uncertainties, it could be acceptable to use a relatively small database of ramp tests to assess the code's prediction in this area.

4.5.2 Methodologies

The methodology for performing the fuel system safety analysis consists of

1. Identification of functional requirements for the fuel and assembly.
2. Identification of limits for each functional requirement.
3. Identification of code or other approach that will be used to assess performance against functional requirement.
4. Identification of approach to demonstrate high level of confidence that design will not exceed functional requirements:
    a. Selection of power histories to be considered
    b. Identification of uncertainties in operational parameters
    c. Identification of fabrication uncertainties
    d. Identification of modeling uncertainties
    e. Approach to quantify an upper tolerance level based on identified uncertainties.

The identification of functional requirements for the fuel and assembly and the limits for each are discussed in Section 4.1. The material property updates and the code assessment has been discussed in Sections 4.1 and 4.5.1. No further methodology change is anticipated as far as the use of codes is considered.

The identification of operational parameters such as rod power, coolant flow rate, are not expected to be impacted by the implementation of FeCrAl cladding.

The identification of fabrication uncertainties will be taken from uncertainty specifications on the drawings or from manufacturing data. Although specific values might change, the general approach for obtaining these values is not expected to change.

The identification of modeling uncertainties should be developed during the implementation of new material properties and code assessment. Comparing property data to correlations and code predictions to measurements should allow for the appropriate development of acceptable modeling uncertainties.

Existing approaches to calculate upper tolerance levels are robust and should be acceptable to perform these calculations for FeCrAl cladding given that the activities discussed above are rigorously performed.

5.0 Conclusions

FeCrAl alloys consist of iron (Fe), chromium (Cr), and aluminum (Al) with minor alloying additions for various purposes. The impact of these various alloying additions is discussed in Section 3.1. The different performance characteristics of the variants are discussed in Section 4.3 and this report concludes an applicant would need to provide data from their specific FeCrAl alloy in a licensing submittal as some properties may be composition dependent.

New damage mechanisms were identified in Section 4.2 and include:

1. Radiation effects on FeCrAl and specifically the neutron activation of Cr-50 and Al-27, which might require a coolant chemistry surveillance program
2. Galvanic corrosion, which occurs between two dissimilar metals. It should be confirmed that the FeCrAl/Zr, FeCrAl/Inconel, and FeCrAl/SS-304 couples do not result in galvanic corrosion in an irradiation environment
3. Defects, introduced in the manufacturing process, should be justified based on testing of cladding with similar defect concentrations.

Additionally, the high mobility of tritium in FeCrAl results in the ability for it to permeate from the fuel, through the cladding, to the coolant, potentially causing dose concerns during plant operation.

Currently available data suggest that for FeCrAl cladding, the increased oxidation resistance minimizes or eliminates the occurrence of ballooning and burst of cladding (see Section 4.3.2.3) but additional data is needed to confirm these results. It is also recommended that further testing is completed to determine if there is a compositional dependence for ballooning and burst behavior. Likewise, further study on the composition dependence of oxide formation (both oxide composition and transition temperatures) is needed.

Experiments have shown the high-temperature oxidation and hydrogen generation rates for FeCrAl alloys are significantly reduced compared to Zr-based alloys but recent analysis of the QUENCH-19 test observed that the oxidation kinetics of FeCrAl alloys are complex and more tests are required to explain them.

In addition to the recommended testing for ballooning and burst behavior and high-temperature oxidation and hydrogen generation rates, several data gaps have been identified including data not yet collected from known irradiation tests (Section 4.3.1), data recommended to be collected on unirradiated cladding (Section 4.3.2), and data recommended to be collected on irradiated cladding (Section 4.3.2).

This page intentionally blank.

6.0 References

Ali, Amir F., Jacob P. Gorton, Nicholas R. Brown, Kurt A. Terrani, Colby B. Jensen, Youho Lee, and Edward D. Blandford. 2018. “Surface Wettability and Pool Boiling Critical Heat Flux of Accident Tolerant Fuel Cladding-FeCrAl Alloys.” *Nuclear Enginering and Design* 338: 218–31.

ASME. 2017. “Boiler and Pressure Vessel Code.”.

Bays, Samuel E., Gilles J. Youinou, Misti Lillo, and Paul Gilbreath. 2018. “ATR Compendium: Irradtiation Test Capabilities.” *Nuclear Technology* 201 (3): 191–208.

Bell, J. T., R. A. Strehlow, J. D. Redman, and F. J. Smith. 1979. “Tritium Permeation Through Steam Generator Materials.” CONF-790803--38.

Berthomé, G., E. N'Dah, Y. Wouters, and A. Galerie. 2005. “Temperature Dependence of Metastable Alumina Formation During Thermal Oxidation of FeCrAl Foils.” *Materials and Corrosion* 56 (6): 389–92.

Brown, Nicholas R., Benton E. Garrison, Richard R. Lowden, M. Nedim Cinbiz, and Kory D. Linton. 2020. “Mechanical Failure of Fresh Nuclear Grade Iron-Chromium-Aluminum (FeCrAl) Cladding Under Simulated Hot Zero Power Reactivity Initiated Accident Conditions.” *Journal of Nuclear Materials* 539: 1–6.

Cappia, Fabiola. 2019. “Post-Irradiation Examinations of Accident Tolerant Fuel Candidates with Iron-Alloy Cladding.” INL/EXT-19-56583.

——— . 2020. E-mail, August 18.

Cappia, Fabiola, and Jason M. Harp. 2019. “Postirradiation Examination of the ATF-1 Experiments - 2019 Status.” INL/EXT-19-55645.

Chen, Xiang, Kevin G. Field, Dalong Zhang, Caleb P. Massey, Kory D. Linton, Janet P. Robertson, and Andrew T. Nelson. 2019. “Post-Irradiation Fracture Toughness Characterization of Generation II FeCrAl Alloys.” ORNL/TM-2019/1391.

Collier, J., and J. Thome. 1994. *Convective Boiling and Condensation.* 3rd. Oxford, England: Oxford University Press.

Dolley, Evan, Michael Schuster, Cole Crawford, and Raul B. Rebak. 2018. “Mechanical Behavior of FeCrAl and Other Alloys Following Exposure to LOCA Conditions Plus Quenching.” In *Proceedings of the 18th International Conference on Environmental Degradation of Materials in Nuclear Power Systems - Water Reactors*, 185–200.

Eighth EPRI/INL/DOE Joint Workshop on Accident Tolerant Fuel: Fuel Reliability Program Winter Technical Advisory Committee Meeting. 2019.

EPRI. 2019. “Accident-Tolerant Fuel Valuation: Safety and Economic Benefits (Revision 1).” 3002015091.

Fawcett, Russ M. 2019. “GE/GNF ATF Program Update.” 2019.

Field, Kevin G. 2018. “Handbook on the Material Properties of FeCrAl Alloys for Nuclear Power Production Applications: FY18 Version, Revision 1.1.” ORNL/SPR-2018/905.

Field, Kevin G., Samuel A. Briggs, Kumar Sridharan, Richard H. Howard, and Yukinori Yamamoto. 2017. “Mechanical Properties of Neuron-Irradiated Model and Commercial FeCrAl Alloys.” *Journal of Nuclear Materials* 489: 118–28.

Field, Kevin G., Xunxiang Hu, Kenneth C. Littrell, Yukinori Yamamoto, and Lance L. Snead. 2015. “Radiation Tolerance of Neutron-Irradiated Model Fe-Cr-Al Alloys.” *Journal of Nuclear Materials* 465: 746–55.

Garner, F. A., M. B. Toloczko, and B. H. Sencer. 2000. “Comparison of Swelling and Irradiation Creep Behavior of Fcc-Austenitic and Bcc-Ferritic/martensitic Alloys at High Neutron Exposure.” *Journal of Nuclear Materials* 276: 123–42.

GE. 1966. “Fifth Annual Report High-Temperature Materials Programs: Part A.” GEMP-400A.

GE. 1968. “Seventh Annual Report - AEC Fuels and Materials Development Program.” GEMP-1400A.

Geelhood, K. J., C. Beyer, and M. Cunningham. 2004. “Modifications to FRAPTRAN to Predict Fuel Rod Failures Due Tto PCMI During RIA-Type Accidents.” In *2004 International Meeting on LWR Fuel Performance*.

Geelhood, K. J., W. G. Luscher, I. E. Porter, L. Kyriazidis, C. E. Goodson, and E. E. Torres. 2020. “MatLib-1.0: Nuclear Material Properties Library.” PNNL-29728.

“Global Nuclear Fuel Accident Tolerant Fuel Assemblies Installed in U.S. Plant.” 2020. News release. January 14, 2020.

Goldner, F. J., W. McCaughey, S. L. Hayes, D. M. Wachs, Kurt A. Terrani, A. T. Nelson, K. J. McClellan, and C. R. Stanek. 2019. “The U.S. Accident Tolerant Fuels Program - a National Initiative Coming of Age.” 2019, 385–92.

Gussev, M. N., E. Cakmak, and Kevin G. Field. 2018. “Impact of Neutron Irradiation on Mechanical Performance of FeCrAl Alloy Laser-Beam Weldments.” *Journal of Nuclear Materials* 504: 221–33.

Harp, Jason M., Fabiola Cappia, and Luca Capriotti. 2018. “Postirradiation Examination of the ATF-1 Experiments - 2018 Status: Rev. 0.” INL/EXT-18-51497.

He, Yang, Jianhua Liu, Shengtao Qiu, Zhenqiang Deng, Yindong Yang, and Alexander McLean. 2018. “Microstructure and High Temperature Mechanical Properties of as-Cast FeCrAl Alloys.” *Materials Science & Engineering A* 726: 56–63.

Jang, Hun. 2019. “ATF R&D Program Review in Korea.” 2019.

Joshi, P., B. Kombaiah, M. Nedim Cinbiz, and K. L. Murty. 2020. “Characterization of Stress-Rupture Behavior of Nuclear-Grade C26M2 FeCrAl Alloy for Accident-Tolerant Fuel Cladding via Burst Testing.” *Materials Science & Engineering A* 791.

Kandlikar, Satish G. 2001. “A Theoretical Model to Predict Pool Boiling CHF Incorporating Effects of Contact Angle and Orientation.” *Journal of Heat Transfer* 123 (6): 1071–79.

Kane, Kenneth, Soon K. Lee, S. B. Bell, Nicholas R. Brown, and Bruce A. Pint. 2020. “Burst Behavior of Nuclear Grade FeCrAl and Zircaloy-2 Fuel Cladding Under Simulated Cyclic Dryout Conditions.” *Journal of Nuclear Materials* 539.

Kanthal. 2019. “Kanthal APMT Datasheet.”.

Kim, Hyun-Gil, Il-Hyun Kim, Yang-Il Jung, Dong-Jun Park, Jung-Hwan Park, Young-Ho Lee, and Byung-Kwon Choi. 2019. “Status of ATF Cladding Development at KAERI.” 2019.

Kim, Sungyu, Joonho Moon, and Chi Bum Bahn. 2019. “Effects of Yttrium on High Temperature Steam Oxidation Behavior of FeCrAl-Y Alloy.” 2019, 621–26.

Kim, Taeyong, Seung Chang Yoo, Inyoung Son, Junhyuk Ham, Yunju Lee, Sungyu Kim, Chi Bum Bahn, and Ji Hyun Kim. 2019. “Effect of Yttrium Addition on the Corrosion Behavior of FeCrAl Alloys in Simulated Primary Water Condition.” 2019, 503–11.

Kimura, A., S. Yuzawa, Y. Yamasaki, K. Yabuuchi, Kan Sakamoto, S. Ukai, A. Yamaji, K. Kusagaya, T. Kondo, and S. Yamashita. 2018. “Welding Technology R&D of Japanese Accident Tolerant FeCrAl-ODS Fuel Claddings for BWRs (2).” 2018.

Le Coq, Annabelle G., Rodger C. Martin, and Kory D. Linton. 2019. “Transportation Planning for Irradiated Fuel-Cladding and Integral FeCrAl Experiments.” ORNL/SPR-2019/1123.

Lee, Soon K., Maolong Liu, Nicholas R. Brown, Kurt A. Terrani, Edward D. Blandford, Heng Ban, Colby B. Jensen, and Youho Lee. 2019. “Comparison of Steady and Transient Flow Boiling Critical Heat Flux for FeCrAl Accident Tolerant Fuel Cladding Alloy, Zircaloy, and Inconel.” *International Journal of Heat and Mass Transfer* 132: 643–54.

Lee, Young-Ho, and Thak Sang Byun. 2015. “A Comparitive Study on the Wear Behaviors of Cladding Candidates for Accident-Tolerant Fuel.” *Journal of Nuclear Materials* 465: 857–65.

Liu, Tong, Jiaxiang Xue, Rui Li, Lei Li, Daxi Guo, Qiang Zhang, and Duoting Xu. 2018. “The Research on Accident Tolerant Fuel in CGN.” 2018.

Massey, Caleb P., Kurt A. Terrani, Sebastien N. Dryepondt, and Bruce A. Pint. 2016. “Cladding Burst Behavior of Fe-Based Alloys Under LOCA.” *Journal of Nuclear Materials* 470: 128–38.

Murdock, Christopher J. 2018. “Accident Tolerant Fuels Series 1 (ATF-1) Irradiation Testing FY 2018 Status Report.” INL/EXT-18-51584.

O'Donnell, W., and B. Langer. 1964. “Fatigue Design Basis for Zircaloy Components.” *Nuclear Science and Engineering*, 1–12.

OECD-NEA. 2018. “State-of-the-Art Report on Light Water Reactor Accident-Tolerant Fuels.” NEA No. 7317.

O'Hanley, Harry, Carolyn Coyle, Jacopo Buongiorno, Tom McKrell, Lin-Wen Hu, Michael Rubner, and Robert Cohen. 2013. “Separate Effects of Surface Roughness, Wettability, and Porosity on the Boiling Critical Heat Flux.” *Applied Physics Letters* 103 (2): 1–5.

Pint, Bruce A., Kurt A. Terrani, Yukinori Yamamoto, and Lance L. Snead. 2015. “Material Selection for Accident Tolerant Fuel Cladding.” *Metallurgical and Materials Transactions E* 2E: 190–96.

Porter, I. E., K. J. Geelhood, D. Richmond, D. V. Colameco, T. J. Zipperer, E. E. Torres, W. G. Luscher, L. Kyriazidis, and C. E. Goodson. 2020. “FAST-1.0: Integral Assessment.” PNNL-29727.

Powers, D. A., and R. O. Meyer. 1980. “Cladding Swelling and Rupture Models for LOCA Analysis.” NUREG-0630.

Raiman, Stephen S., Kevin G. Field, Raul B. Rebak, Yukinori Yamamoto, and Kurt A. Terrani. 2020. “Hydrothermal Corrosion of 2nd Generation FeCrAl Alloys for Accident Tolerant Fuel Cladding.” *Journal of Nuclear Materials* 536.

Rebak, Raul B. 2018a. “Versatile Oxide Films Protect FeCrAl Alloys Under Normal Operation and Accident Conditions in Light Water Power Reactors.” *JOM* 70 (2).

Rebak, Raul B., V. K. Gupta, M. Brobnjak, D. J. Keck, and Evan Dolley. 2018b. “Overcoming Sensitization in Welds Using FeCrAl Alloys.” 2018.

Rebak, Raul B., Timothy B. Jurewicz, and Young-Jin Kim. 2017. “Oxidation Resistance of FeCrAl in Simulated BWR and PWR Water Chemistries.” 2017.

Rebak, Raul B., Timothy B. Jurewicz, Michael Larsen, and Kan Sakamoto. 2019. “Immersion Testing of FeCrAl Tubes Under Simulated Light Water Nuclear Reactor Normal Operation Conditions.” 2019, 485–93.

Rebak, Raul B., Kurt A. Terrani, and Russ M. Fawcett. 2016. “FeCrAl Alloys for Accident Tolerant Fuel Cladding in Light Water Reactors.” In *ASME 2016 Pressure Vessels & Piping Conference*.

Richardson, Kate, and Heather Medema. 2019. “Advanced Fuels Campaign 2019 Accomplishments.” INL/EXT 19-56259.

Robb, Kevin R., Michael Howell, and Larry J. Ott. 2018. “Design and Analysis of Oxidation Tests to Inform FeCrAl ATF Severe Accident Models.” ORNL/SPR-2018/893.

Sakamoto, Kan, Y. Miura, S. Ukai, A. Kimura, A. Yamaji, K. Kusagaya, and S. Yamashita. 2019. “Recent Progress in Development of Accident Tolerant FeCrAl-ODS Fuel Claddings for BWRs in Japan.” 2019, 197–205.

Sakamoto, Kan, A. Ouchi, A. Suzuki, T. Higuchi, M. Hirai, N. Oono, and S. Ukai. 2016. “Development of Ce-Type FeCrAl-ODS Ferritic Steel to Accident Tolerant Fuel for BWRs.” In *Top Fuel 2016*, 673–80.

Sato, T., Y. Nakahara, F. Ueno, S. Yamashita, and Kan Sakamoto. 2018. “Effects of Dissolved Oxygen and Ion Irradiation on the Corrosion of FeCrAl-ODS in High-Temperature Water Simulating BWR Operating Conditions.” 2018.

Schmidt, Rodney C., Laura P. Swiler, Danielle M. Perez, and Richard L. Williamson. 2014. “Sensitivity Analysis of the Gap Heat Transfer Model in BISON.” SAND2014-18550.

Schuster, Michael, Cole Crawford, and Raul B. Rebak. 2017. “Fresh Water Quenching of Alloys of Nuclear Interest Including FeCrAl for Accident Tolerant Fuel Cladding.” 2017.

Special Metals. “INCOLOY Alloy MA956.”.

Stuckert, J., Mirco Grosse, Martin Steinbrück, and Kurt A. Terrani. 2019. “Results of the Bundle Test QUENCH-19 with FeCrAl Claddings.” 2019, 922–27.

Szőke, R., M. A. McGrath, and P. Bennett. 2017. “Dimensional Behaviour Testing of Accident Tolerant Fuel (ATF) In the Halden Reactor.” 2017.

Takahatake, Y., H. Ambai, Y. Sano, M. Takeuchi, K. Koizumi, Kan Sakamoto, and S. Yamashita. 2018. “Corrosion Behaviour of FeCrAl-ODS Steels in Nitric Acid Solutions with Several Temperatures.” 2018.

Takata, Y., S. Hidaka, M. Masuda, and T. Ito. 2003. “Pool Boiling on a Superhydrophilic Surface.” *International Journal of Energy Research* 27: 111–19.

Tang, Chongchong, Adrian Jianu, Martin Steinbrück, Mirco Grosse, Alfons Weisenburger, and Hans Juergen Seifert. 2018. “Influence of Composition and Heating Schedules on Compatibility of FeCrAl Alloys with High-Temperature Steam.” *Journal of Nuclear Materials* 511: 496–507.

Terrani, Kurt A. 2018. “Accident Tolerant Fuel Cladding Development: Promise, Status, and Challenges.” *Journal of Nuclear Materials* 501: 13–30.

Terrani, Kurt A., Bruce A. Pint, Young-Jin Kim, K. A. Unocic, Y. Yang, C. M. Silva, H. M. Meyer III, and Raul B. Rebak. 2016. “Uniform Corrosion of FeCrAl Alloys in LWR Coolant Environments.” *Journal of Nuclear Materials* 479: 36–47.

U.S. Congress. 2011. “Energy and Water Development Appropriations Bill, 2012: To Accompany H.R. 2354.” S. Rep. 112-75.

U.S. NRC. 2007. “Standard Review Plan: Section 4.2, Fuel System Design.” NUREG-0800, Rev. 3.

U.S. NRC. 2017. “Acceptance Criteria for Emergency Core Cooling Systems for Light-Water Nuclear Power Reactors.” 10 CFR 50.46.

Wang, Peng, Slavica Grdanovska, David M. Bartels, and Gary S. Was. 2020. “Effect of Radiation Damage and Water Radiolysis on Corrosion of FeCrAl Alloys in Hydrogenated Water.” *Journal of Nuclear Materials* 533.

Weatherford, R. 1963. “Nucleate Boiling Characteristics and Critical Heat Flux Occurrence in Sub-Cooled Axial Flow Water Systems.” ANL-6675.

Winter, Thomas C., Richard W. Neu, Preet M. Singh, Lynne E. Kolaya, and Chaitanya S. Deo. 2018. “Fretting Wear Comparison of Cladding Materials for Reactor Fuel Cladding Application.” *Journal of Nuclear Materials* 508: 505–15.

Wukusick, C. S. 1966. *The Physical Metallurgy and Oxidation Behavior of Fe-Cr-Al-Y Alloys.* Cincinnati, OH.

Yamamoto, Yukinori, Kevin G. Field, Bruce A. Pint, Raul B. Rebak, and Russ M. Fawcett. 2020. “Development of Nuclear Grade Wrought FeCrAl Alloys for Accident Tolerant Fuel Cladding.” TMS2020 - 149th Annual Meeting and Exhibition, San Diego, CA, 2020.

Yamamoto, Yukinori, Kenneth Kane, Bruce A. Pint, Artem Trofimov, and Hsin Wang. 2019. “Report on Exploration of New FeCrAl Heat Variants with Improved Properties.” ORNL/TM-2019/1290.

Yamamoto, Yukinori, Bruce A. Pint, Kurt A. Terrani, Kevin G. Field, Y. Yang, and Lance L. Snead. 2015. “Development and Property Evaluation of Nuclear Grade Wrought FeCrAl Fuel Cladding for Light Water Reactors.” *Journal of Nuclear Materials* 467: 703–16.

Yamashita, S., I. Ioka, Y. Nemoto, T. Kawanishi, M. Kurata, Y. Kaji, T. Fukahori et al. 2019. “Overview of Accident-Tolerant Fuel R&D Program in Japan.” 2019, 206–16.

Yang, J. H., Hyun-Gil Kim, D.-J. Kim, C. H. Shin, and W.-J. Kim. 2019. “Advances in ATF R&D at KAERI.” 2019.

Yano, Y., T. Tanno, H. Oka, S. Ohtsuka, T. Inoue, S. Kato, T. Furukawa et al. 2017. “Ultra-High Temperature Tensile Properties of ODS Steel Claddings Under Severe Accident Conditions.” *Journal of Nuclear Materials* (487): 229–37.

Zhang, Zhexian, Tarik A. Saleh, Stuart A. Maloy, and Osman Anderoglu. 2020. “Microstructure Evolution in MA956 Neutron Irradiated in ATR at 328 °C to 4.36 Dpa.” *Journal of Nuclear Materials* 533.

Pacific Northwest National Laboratory

902 Battelle Boulevard
P.O. Box 999
Richland, WA 99354
1-888-375-PNNL (7665)

www.pnnl.gov